HHS Public Access

Author manuscript

Wiley Interdiscip Rev Nanomed Nanobiotechnol. Author manuscript; available in PMC 2018 January 01.

Published in final edited form as:

Wiley Interdiscip Rev Nanomed Nanobiotechnol. 2017 January ; 9(1): . doi:10.1002/wnan.1412.

Detection and Treatment of Atherosclerosis Using Nanoparticles

Jia Zhang[1], **Yujiao Zu**[1], **Chathurika S. Dhanasekara**[1], **Jun Li**[2], **Dayong Wu**[3], **Zhaoyang Fan**[4], and **Shu Wang**[1,*]

[1]Department of Nutritional Sciences, Texas Tech University, Lubbock, TX 79409, USA.

[2]Laboratory Animal Center, Peking University, Beijing, PR China.

[3]Nutritional Immunology Laboratory, Jean Mayer Human Nutrition Research Center on Aging, Tufts University, Boston, MA 02111, USA.

[4]Department of Electrical and Computer Engineering and Nano Tech Center, Texas Tech University, Lubbock, TX 79409, USA.

Abstract

Atherosclerosis is the key pathogenesis of cardiovascular disease, which is a silent killer and a leading cause of death in the United States. Atherosclerosis starts with the adhesion of inflammatory monocytes on the activated endothelial cells in response to inflammatory stimuli. These monocytes can further migrate into the intimal layer of the blood vessel where they are differentiate into macrophages, which take up oxidized low-density lipoproteins and release inflammatory factors to amplify the local inflammatory response. After accumulation of cholesterol, the lipid-laden macrophages are transformed into foam cells, the hallmark of the early stage of atherosclerosis. Foam cells can die from apoptosis or necrosis, the intracellular lipid is deposed in the artery wall forming lesions. The angiogenesis for nurturing cells is enhanced during lesion development. Proteases released from macrophages, foam cells and other cells degrade the fibrous cap of the lesion, resulting in rupture of the lesion and subsequent thrombus formation. Thrombi can block blood circulation, which represents a major cause of acute heart events and stroke. There are generally no symptoms in the early stages of atherosclerosis. Current detection techniques cannot easily, safely and effectively detect the lesions in the early stages, nor can they characterize the lesion feature such as the vulnerability. While the available therapeutic modalities cannot target specific molecules, cells, and processes in the lesions, nanoparticles appear to have a promising potential in improving atherosclerosis detection and treatment via targeting the intimal macrophages, foam cells, endothelial cells, angiogenesis, proteolysis, apoptosis, and thrombosis. Indeed, many nanoparticles have been developed in improving blood lipid profile and decreasing inflammatory response for enhancing therapeutic efficacy of drugs and decreasing their side effects.

[*]**To whom correspondence should be addressed**: Dr. Shu Wang, Department of Nutritional Sciences, Texas Tech University, 1301 Akron Avenue, Lubbock, TX 79409-1240, USA, Telephone number: (806) 834-4050, shu.wang@ttu.edu.

All authors have no conflict of interest in relation to this study.

INTRODUCTION

Atherosclerosis is a disease characterized by a process of building up of lipids, primarily cholesterol, in the artery wall [1, 2]. Atherosclerosis provides a pathological background for developing cardiovascular disease (CVD), the No. 1 killer in the United States. The structure of arteries from the inner cavity to the outermost layer is lumen, an intimal layer composed of an endothelial cell monolayer and underneath intima, a media layer composed of multiple layers of smooth muscle cells and connective tissues, and an adventitia layer composed of connective tissues[3].

Cholesterol accumulation and deposition in the arterial wall and subsequent narrowing of the blood vessel lumen were considered as a sole cause of atherosclerosis in the past century[1]. In the past two decades, research in both preclinical and clinical areas has suggested that inflammation integrated with dyslipidemia plays an important role in the development of atherosclerosis[4]. The endothelial cells are important in maintaining blood vessel integrity and permeability, adhesion molecule expression, leukocyte recruitment, and blood clotting[5]. Under normal circumstance, vascular endothelial cells resist the adhesion of circulating immune cells on them[6]. Atherogenic stimuli such as inflammation, hypertension, cigarette smoking, hyperlipidemia, especially hypercholesterolemia, and/or hyperglycemia increase their expression of adhesion molecules, disrupt the monolayer structure of endothelial cells, increase blood vessel wall permeability, and enhance their release of inflammatory factors[1]. Although many immune cells contribute to atherosclerotic lesion formation, intimal macrophages play a critical role in the development of atherosclerosis[4, 7]. After monocytes attach on the endothelial cells via binding to adhesion molecules, chemokines, especially monocyte chemoattractant protein 1 (MCP-1), direct monocytes migration into the intimal layer where they differentiate into macrophages. Lesion-resident macrophages recruit more monocytes into the evolving intimal lesion via secreting more MCP-1 and other inflammatory factors. When cholesterol influx is more than efflux, cholesterol is accumulated in the intimal macrophages. The lipid-laden macrophages are called foam cells, which are the hallmark of atherosclerosis. After foam cells die from apoptosis and necrosis, the cellular lipids are deposited in the artery wall leading to formation of atherosclerotic lesions. If the inflammatory condition and dyslipidemia persist, the advanced atherosclerotic lesion will be formed, which is characterized by a large lipid, primarily cholesterol, core, proliferated smooth muscle cells and remodeled extracellular matrix[8].

Rupture of vulnerable lesions (plaques) followed by thrombi formation accounts for a majority of coronary events and/or sudden deaths[9–12]. Vulnerable lesions are characterized by macrophage-dense inflammation, large lipid cores, thin fibrous caps and few smooth muscle cells[11, 13]. Intimal macrophage accumulation promotes the development of vulnerable lesions by producing reactive oxygen species to increase the intimal levels of oxidized low density lipoproteins (oxLDL) and further foam cell formation; by producing matrix metalloproteinases and other proteases to degrade the extracellular matrix and fibrous caps; by releasing tissue factors to promote thrombus formation; by secreting pro-inflammatory cytokines to amplify the lesion inflammatory response[6, 14, 15]. Current imaging and diagnostic techniques can detect stenotic lesions, but they cannot detect early-stage lesions and disclose the lesion biological aspects such as vulnerability[16]. Current

preventive and therapeutic modalities focus on improving blood lipid profile, inhibiting thrombus formation, and decreasing blood pressure, but the treatment cannot directly target the atherosclerotic lesion[17].

Since most biological processes, including atherogenesis, occur at the nanoscale, nanotechnology provides a promising opportunity for molecular imaging and targeted treatment of atherosclerosis[18]. Nanoparticles can increase the stability, aqueous solubility and absorption of diagnostic agents or therapeutic compounds, prolong their circulation time, enable high binding and uptake efficiency in the target cells (or tissue) over other cells (or tissue), protect them from degradation by enzymes in tissues and physiological fluids, reduce their side effects and toxicity[19]. Nanomedicine has gained tremendous attention in cancer therapy for more than 30 years. In contrast, however, its application in atherosclerosis is much less studied even given the fact that atherosclerosis is the key pathogenesis factor for developing CVD, a top cause of mortality worldwide. In the earliest studies published in 2000 and 2001, two studies reported that fibrin-targeted nanoparticles detected thrombi and perhaps vulnerable lesions[20, 21]. Meanwhile, ultrasmall superparamagnetic particles of iron oxide were used for imaging atherosclerotic lesions in an animal model[22]. Shortly later, other investigators used iron oxide nanoparticles with anti-human E-selectin fragments conjugated on their surface to detect endothelial cells[23], or used alpha(v)beta3 ($\alpha_v\beta_3$) integrin-targeted nanoparticles to image angiogenesis in early-stage atherosclerosis[24]. Last decade has seen a fast development in using nanoparticle technique as tool for molecular imaging of atherosclerotic lesion[25, 26]. Since intimal macrophages are critical cells in atherosclerosis development, and can engulf nanoparticles by phagocytosis, they are the major nanoparticle targets in this research field[27–29]. Currently, majority of studies are in the preclinical stage as we summarized in a chronological manner (Table 1–5), while only a limited number of clinical studies were conducted by using passive macrophage-targeted nanoparticles and listed in Table 1.

In this review, we are focused on the nanoparticle-mediated detection and treatment of atherosclerosis via targeting intimal macrophages, foam cells, endothelial cells, and processes of neoangiogenesis, proteolysis, apoptosis, and thrombosis (Figure 1). Nanoparticle-mediated low density lipoproteins (LDL) and HDL metabolism and anti-inflammation will be addressed at the end of this review.

STRUCTURAL AND FUNCTIONAL IMAGING OF ATHEROSCLEROSIS

Structural Imaging

Several imaging modalities have been used in visualizing the vascular structure of atherosclerosis including the lesion volume and fibrous cap thickness [30]. Magnetic resonance imaging/angiography (MRI/MRA) is a commonly used method, which utilizes gadolinium (Gd) chelates/nanoparticles, superparamagnetic iron oxide probes (SPIO), ultrasmall superparamagnetic iron oxide (USPIO) as contrast enhancement with resolution of 10–100 μm to visualize the structure of atherosclerotic lesions[31]. Computed tomography (CT) is a method utilizing iodinated molecules as imaging moieties and high-resolution X-ray as technology with resolution of 50 μm for clinical or preclinical imaging[32]. Positron emission tomography (PET)/Single-photon emission computed tomography (SPECT) as an

approach is increasingly popular by using imaging moieties such as ^{18}F, ^{64}Cu, ^{11}C Tracers/ ^{99m}Tc,$^{123/124/125/131}$I, ^{111}In tracers and nuclear technology with resolution of ~2 μm[32]. Angiography (X-ray-based fluoroscopy and iodinated molecules as contrast agent), optical coherence tomography (OCT)/optical frequency domain imaging (OFDI), optical angioscopy, intravascular ultrasound are commonly used invasive approaches to detect atherosclerotic lesions[33].

Functional Imaging

Imaging of specific cells or components in lesions can disclose lesion biology and feature, especially vulnerability, which can help prevent major cardiovascular events[34]. By incorporating peptides, antibodies or other ligands on its surface, a nanoparticle can target lesion components (i.e. collagen, proteinases, reactive oxygen species) and cells[17, 35]. Diagnostic dyes or contrast agents are incorporated in the nanoparticles, which can be detected using modalities including MRI, PET/SPECT, CT, optical near infrared fluoroscopy (NIRF)[36, 37]. Although fluorescence imaging cannot be used in clinical research because of short penetration, it is a good approach to image atherosclerosis in small animal models. Dysfunctional endothelial cells can be visualized by using nanoparticles, conjugated with specific ligands allowing to target adhesion molecules[38, 39]. Macrophages and foam cells are the most abundant inflammatory cells in atherosclerotic lesions. Intimal macrophages and foam cells have phagocytic activities, express scavenger receptors (i.e., CD36, LOX-1, MSR1) and also release reactive oxygen species (oxidized epitopes) and matrix-degrading proteases (i.e., matrix metalloproteinases and cathepsins); thus all these features can serve as potential targets to visualize macrophages and foam cells and to estimate their oxidative and inflammatory activities [40, 41]. Fibrin and factor XIII can be used to target thrombosis[42]. The $\alpha_v\beta_3$ Integrin can be used to visualize lesion neoangiogenesis[24, 43]. Abundance and distribution of those cells and the key active components in lesions provide valuable information beyond lesion volume[34, 44]. The events such as inflammation, especially neoangiogenesis, fibrous cap degradation, oxidative stress, are critical for subsequent selection of preventive and therapeutic modalities.

NANOPARTICLES TARGET ATHEROSCLEROTIC LESIONS

When an atherosclerotic lesion is developing, the permeability of the endothelial layer of arterial wall increases, which allows more lipoproteins and small particles such as nanoparticles to migrate into the intimal layer[45, 46]. Expanding atherosclerotic lesions requires oxygen and nutrients to allow neoangiogenesis occur[47]. The neovessels are prone to be leaky and fragile[47] resulting in increased permeability and retention (EPR), further promoting lesion expansion. Nanoparticle migration into atherosclerotic lesions via the EPR effect is considered as a non-specific targeting process[17]. Recognition of nanoparticles by their binding to the specific cells or molecules in the lesions via their surface ligands are thought to be an active targeting process[17].

Intimal Macrophages and Foam Cells

Macrophages and their derived lipid-laden foam cells are determinant cells of atherosclerotic lesions due to their ability to accumulate lipids and increase inflammatory responses[2].

Recruitment and deposition of macrophages into the artery wall occur prior to lesion development[48]. Additionally, accumulation and activation of intimal macrophages positively correlates with lesion size[49]. The recruitment of blood monocytes followed by subsequent differentiation to intimal macrophages and their proliferation *in situ* increase lesion macrophage numbers, while macrophage emigration or death decreases their numbers[2, 4] The content of intimal macrophages depends on the kinetic balance between the above processes [2]. Targeting intimal macrophages and foam cells is a promising avenue for detection and treatment of atherosclerosis.

Macrophages are phagocytic cells, and they eat up dying or dead cells and foreign particles or microbes. Iron oxide nanoparticles have been widely used to detect intimal macrophages by MRI, because like most other foreign particles, iron oxide particles can be taken up by macrophages through their phagocytic function of macrophages in the whole body[28, 29] (Table 1). There are two major types of iron oxide nanoparticles are superparamagnetic iron oxide (SPIO) nanoparticles with size of more than 50 nm in diameter and ultrasmall SPIO (USPIO) nanoparticles with size of between 18 nm to 50 nm in diameter[51]. Magnetic nanoparticles used in MRI usually contain iron cores such as magnetite (Fe_3O_4) and maghemite (γ-Fe_2O_3), and their surface is modified by hydrophilic coating such as dextrans (most commonly), carboxydextran, carboxymethylated dextran, chitosan, starches, polyvinyl alcohol, poly(ethylene glycerol) (PEG), polylactic-co-glycolic acid, polymethyl methacrylate, polyacrylic acid and polyvinyl pyrrolidone[30].

Intimal macrophages bind and take up native LDL and oxLDL cholesterol via their scavenger receptors including the CD36 receptor, macrophage scavenger receptor 1 (MSR1/CD204/SR-A1), lectin-like oxidized LDL receptor-1 (LOX-1), SR-B1, CD68, macrophage receptor with collagenous structure (MARCO) among others[33, 52]. CD36 is an 88-kDa transmembrane receptor belonging to the class B scavenger receptor family[53, 54]. Studies performed in mice suggest that CD36 is more important than other macrophage scavenger receptors in the process of oxLDL uptake, foam cell formation, and atherosclerotic lesion development[55–57]. Injection of CD36-null macrophages into atherosclerosis-prone mice profoundly reduced the atherosclerotic lesion formation, while reintroduction of macrophages with CD36 increased the lesion formation by 2-fold[58]. Blockage of oxLDL binding site of CD36 using a peptide ligand reduced lesion size by more than 50% in apolipoprotein E null (apoE−/−) mice[59]. Furthermore, CD36 correlates well with lesion severity[56, 57, 60]. Since CD36 can recognize and bind to oxLDL, one or more components of oxLDL must be ligand(s) for CD36. Terpstra V and Bird DA et al. extracted the lipids from oxLDL exhaustively by using a chloroform and methanol mixture, and reconstituted these lipids into microemulsions. They found these microemulsions competed effectively for the binding of intact oxLDL to the macrophages. However, microemulsions containing lipids from native LDL did not show the effect[61, 62]. Oxidized phospholipids naturally found on oxLDL are enriched in atherosclerotic lesions of animals[63, 64]. Therefore, they seem to be the most likely ligands for binding oxLDL to CD36. On the surface of oxLDL, hydrophilic head and *sn*-2 acyl group of oxidized phosphatidylcholines protrude to the aqueous phase, resulting in a lipid whisker model[65]. The protruded and oxidized *sn*-2 acyl group incorporating a terminal γ-hydroxy (or oxo)-α,β-unsaturated carbonyl is critical for its high binding affinity to CD36[64, 66, 67]. Podrez EA et al. compared the binding affinity of different

oxidized phosphatidylcholines to CD36[64]. 1-(Palmitoyl)-2-(5-keto-6-octene-dioyl)phosphatidylcholine (KOdiA-PC), 1-palmitoyl-2-(4-keto-dodec-3-ene-dioyl)phosphatidylcholine (KDdiA-PC) and 9-keto-12-oxo-10-dodecenoic acid of 2-lysophosphatidylcholine (KODA-PC) have the highest binding affinity to CD36 among 14 tested oxidized phosphatidylcholines[64]. We made liposome-like nanoparticles using phosphatidylcholine and KOdiA-PC[27]. We intravenously injected those CD36-targeted nanoparticles carrying KOdiA-PC into LDL receptor null (LDLr−/−) mice, and found that those nanoparticles can target intimal macrophages via binding to their CD36 receptors[27]. CD36-targeted nanoparticles had a higher binding affinity to mouse and human macrophages than non-targeted nanoparticles. When we knocked down CD36 using small interfering RNA (siRNA), the binding of CD36-targeted nanoparticles to macrophages was diminished[27]. Lipinski MJ et al. incorporated CD36 antibody on the surface of gadolinium (Gd)-containing lipid-based nanoparticles. Phospholipids, Tween 80 and an aliphatic gadolinium complex were used to make the nanoparticles. They found that the CD36-targeted nanoparticles had high uptake by human macrophages in an *in vitro* experiment, increased signal intensity in human atherosclerotic lesions via binding to intimal macrophages in an *ex vivo* experiment[68].

LOX-1 is a 52 KDa type II membrane receptor. LOX-1 expression on intimal macrophages positively correlates with atherosclerotic lesion instability and vulnerability[36]. Wen S et al conjugated LOX-1 antibody on the surface of USPIO nanoparticles[36]. Those LOX-1 targeted nanoparticles had higher binding affinity to and uptake by RAW264.7 macrophages than non-targeted nanoparticles. After intravenous administration of nanoparticles into apoE−/− mice, targeted nanoparticles gave signal enhancement of atherosclerotic lesions, especially in the areas enriched with macrophages/foam cells[36]. Besides imaging of the intimal macrophages and atherosclerotic lesions, this approach might also characterize vulnerable atherosclerotic lesions. MSR-1 is another important scavenger receptor involved in macrophage uptake of oxLDL and subsequent foam cell formation[69]. After conjugating peptidic MSR1 ligands or MSR1 antibodies on the nanoparticles, those MSR1-targeted nanoparticles can target atherosclerotic lesions by binding to MSR-1 on intimal macrophages[37, 70, 71]. Other macrophage targeting mechanisms include incorporating apolipoprotein A-1 peptides on high density lipoprotein (HDL)[72]; incorporating phosphatidylserine on nanoparticles for targeting phosphatidylserine receptors on macrophages[52]. Table 1 lists detailed information about different types of macrophage-targeted nanoparticles, and their target mechanisms in published preclinical and clinical research studies.

Targeted delivery of therapeutic compounds, siRNA and others to intimal macrophages represents an innovative and efficient treatment to atherosclerosis (Table 2). Macrophage-targeted therapy can prevent or inhibit lesion development by decreasing lipid accumulation and inflammation. Most of intimal macrophages are differentiated from circulating monocytes of both bone marrow and spleen origin[2]. There are two types of circulating monocytes: inflammatory and non-inflammatory monocytes[2]. Inflammatory monocytes (Ly-6C^{high} in the mouse, CD14^{++}CD16^{-} in human) are differentiated to classical (M1 type) macrophages, which increase inflammatory response[73]. Non-inflammatory monocytes (Ly-6C^{low} in the mouse, CD14$^{+/low}$CD16^{+} in human) are differentiated to alternative (M2

type) macrophages, which decrease inflammatory response[73]. The M2 macrophages are subdivided into three subtypes (M2a, M2b, and M2c), which have functions of Th2 responses, Th2 activation, and immunoregulation, respectively[74]. Different phenotypes of macrophages have different functions[74, 75]. Studies thus far have shown a lack of consensus in describing or defining their macrophage phenotypes[75]. To our knowledge, none of nanoparticles has been developed to identify or target a specific phenotype of macrophages. Inflammatory, but not non-inflammatory, monocytes depend on the CC-chemokine receptor 2 (CCR2) for distribution to the blood vessel wall[73]. Upon binding to CCR2 of inflammatory monocytes, MCP-1 directs their migration into the intimal layer. Increased invasion of inflammatory monocytes critically promote lesion formation, progression and its complications[76]. In contrast, decreased invasion of inflammatory monocytes results in less foam formation and diminished local inflammatory response, which inhibit lesion formation and progression. Decreased expression of CCR2 prevents inflammatory monocyte migration to, and accumulation in the sites of inflammation[73]. Leuschner F et al. developed CCR2 siRNA loaded lipid nanoparticles, which are composed of C12–200, disteroylphosphatidylcholine, cholesterol and PEG–dimyristolglycerol[73]. After systemic administration of those nanoparticles, mRNA and protein expression of CCR2 in inflammatory monocytes were significantly decreased. The CCR2 siRNA loaded lipid nanoparticles decreased the number of inflammatory monocytes by more than 70%, and lowered the migratory capacity of inflammatory monocytes towards MCP-1 by more than 90%. After 3-week intravenous treatment to apoE−/− mice, the number of intimal macrophages was reduced by 82%, which correlated with a 38% reduction of aortic root lesion size[73]. Majmudar MD et al. used polymeric nanoparticles to carry CCR2 siRNA[77]. After administration of those CCR2 siRNA-loaded nanoparticles to apoE−/− mice, they found that more than 75% of nanoparticles were taken up by monocytes/macrophages. Mice treated with CCR2 siRNA-loaded nanoparticles had decreased monocyte invasion and subsequent decreased number of intimal macrophages, which are associated with decreased expression of inflammatory genes in the lesions[77]. McCarthy JR et al. developed a light-activated nanoagent, which can be taken up by intimal macrophages in inflamed atherosclerotic lesions[78]. They induced apoptosis of intimal macrophages using a therapeutic dose of light. Ablation of intimal macrophages might decrease lesion formation via decreasing foam cell formation, and stabilize lesions via lowering inflammation[78]. Most of the above studies did not present deep underlying mechanisms, such as monocyte/macrophage population number, phenotype, their origins, or shift from inflammatory to inflammatory monocyte/macrophage. More intensive and deep investigation in the underlying mechanisms is required in this research field.

Technically, specificity is still not satisfactory as most of targeted nanoparticles target not only intimal macrophages, but other types of cells in the body are also impacted. For example, many “intimal macrophage specific” target molecules including CD36, LOX-1, SR-B1 and other scavenger receptors are also present in other cells, and even the most advanced nanoparticles cannot target a specific monocyte or macrophage phenotype, which render the danger of off-target effects. Future studies are expected to provide more mechanistic insight as to how nanoparticles function to decrease inflammation in the

atherosclerotic lesion, which at least involves abundance, phenotype, origins, and transformation of monocytes/macrophages.

Important macrophage membrane proteins involved in cholesterol efflux are ATP-transporter cassette A1 (ABCA1), ATP-transporter cassette G1 (ABCG1) and scavenger receptor B class 1 (SR-B1)[79]. Ligand activation of liver X receptors (LXR), cholesterol-sensing nuclear receptors, reverses atherosclerosis through regulating lipid absorption, transport and metabolism and suppressing inflammatory response[80]. Both LXRα and LXRβ are expressed in macrophages [81]. GW3965 is one of LXR agonists[81, 82]. Activation of LXR in lesion macrophages can enhance cholesterol efflux and inhibit inflammatory response[80, 83, 84]. ABCA1 promotes free cholesterol efflux from macrophages or foam cells to pre-beta-HDL (pre-β-HDL), which is composed of apolipoprotein AI (apoA-1) and phospholipids[83, 85, 86]. Lecithin cholesterol acyltransferase (LCAT) esterifies free cholesterol on pre-β-HDL into cholesteryl ester, which is then sequestered into the hydrophobic core of HDL[87]. After picking up more cholesterol from peripheral cells, increased cholesteryl ester accumulation enlarges the HDL size and converts it into a mature HDL[87]. Cholesteryl ester in the mature HDL is selectively taken up by liver cells through apoA-1-mediated binding to SR-B1 of hepatocytes[88]. Cholesteryl ester in hepatocytes can be used to synthesize bile acids, and cholesterol and bile acids can be excreted into the bile. If cholesterol and bile acid are not reabsorbed in the intestine, they are eliminated into feces. This process is called reverse cholesterol transport[88]. Even though LXR agonists can increase cholesterol efflux by upregulating ABCA1 and ABCG1 expression on intimal macrophages, they increase liver fat content resulting in a fatty liver disease, which limits the application of LXR agonists including free GW3965 in clinics. Iverson N et al. made a polymeric micelle, which surface amphiphilic macromolecules targeted to macrophage MSR1, resulting in less oxLDL binding and uptake by macrophages[89]. They also encapsulated GW3965 into the micelles, resulting in decreased inflammation and increased cholesterol efflux in macrophages, which was correlated with increased expression of ABCA1, apoA-1 and LXRα[89]. After administering them to Sprague Dawley rats with injured carotid arteries, they found significantly decreased intimal cholesterol content, and inhibited macrophage retention in the inflamed lesion[89]. Another research group encapsulated GW3965 into poly(lactide-co-glycolide)-b-poly(ethylene glycol) (PLGA-b-PEG) nanoparticles[90]. Nanoencapsulated GW3965 had does advantage in inhibiting inflammatory factor expression in macrophages both *in vitro* and *in vivo*. After intravenous injection of those GW3965-encapsulated PLGA-b-PEG nanoparticles into LDLr−/− mice for 2 weeks, the macrophage content in atherosclerotic lesions was dramatically decreased, but liver fat content and blood lipid profile were not changed. Therefore, nanoencapsulation decreased the side effects of free GW3965, and enhanced its therapeutic efficacy[90].

Vascular Endothelial Cells

Endothelium is a continuous monolayer lining in the blood vessel wall[91]. The activation and dysfunction of endothelial cells can be triggered by oxidative stress, dyslipidemia, viral or bacterial infection, inflammation, turbulent blood flow and low shear stress, amongothers[92, 93]. The dysfunctional endothelial cells impact leukocyte adhesion and recruitment, platelet activation, and thrombus formation[91, 94]. Endothelium-targeted

nanoparticles in combination of medical imaging modalities including MRI, PET, and multiple-row detector computed tomography (MDCT) have been developed to visualize atherosclerotic endothelium wall structures and activities[39, 95]. Those nanoparticles can also prevent or treat atherosclerosis via targeted delivery of preventive or therapeutic agents to the activated or dysfunctional endothelial cells[94, 96] (Table 3).

Adhesion molecules contribute to recruitment of inflammatory monocytes into the intimal layer where they differentiate into macrophages, and transform into lipid-laden foam cells, which features the early stage of atherosclerosis. Vascular cell adhesion molecule 1 (VCAM-1), intercellular adhesion molecule 1 (ICAM-1), P- and E-selectin are major adhesion molecules expressed on endothelial cells[97]. VCAM-1 expression is increased on endothelial cells in both early and advanced atherosclerotic lesions, but it is also expressed on activated macrophages and smooth muscle cells[98], VCAM-1 is a potential marker for vascular inflammation and dysfunctional endothelial cells. Tsourkas A et al. conjugated anti-VCAM-1 antibodies on the magneto-optical nanoparticles[99]. The VCAM-1-targeted nanoparticles could detect VCAM-1 expression on the endothelial cells, and label the activated endothelium[99]. Non-targeted nanoparticles had low target specificity to the endothelium[99]. Many VCAM-1 targeting peptides have been selected using the phage display or other approaches[100, 101]. VHSPNKK-modified nanoparticles had 12-fold higher binding affinity to VCAM-1 than VCAM-1 antibodies[100]. Importantly, they had low binding affinity to macrophages[100]. The same research group identified another peptide VHPKQHR, which was used to develop VCAM-1 internalizing nanoparticles (VINP-28)[101]. *In vitro* experiments revealed a 20-fold higher cellular binding and internalization of VINP-28 by VCAM-1 expressing cells than the previous nanoparticles[101]. VINP-28 had high binding affinity to endothelial cells, but low binding affinity to macrophages and smooth muscle cells[102]. After intravenous injection into apoE−/− mice, VINP-28 co-localized with endothelial cells in atherosclerotic lesions, and they detected decreases in VCAM-1 expression in the aortic root in statin-treated mice[101]. VINP-28 also detected endothelial cells and other VCAM-1 expression cells in resected human carotid artery lesion *ex vivo*[101]. Other VCAM-1 ligands have been conjugated to nanoparticles for imaging endothelial cells[38, 39]. Beside VCAM-1, ICAM-1, selectins, stabilin-2, interleukine-4 receptor and other membrane proteins on activated or dysfunctional endothelial cells have been used as targets for designing endothelium-targeted nanoparticles[39, 103, 104].

After intravenous administration, nanoparticles contact endothelial cells of the blood vessel wall. The effects of nanoparticle exposure on endothelium structure, function, activity are gaining considerable attentions. It is crucial to understand endothelial cell functional changes and toxicity and underlying mechanisms upon nanoparticle exposure. Many metal nanoparticles including cobalt, titanium oxide[105], silica[106], zinc oxide[107] and iron oxide[108] nanoparticles significantly upregulated the expression of MCP-1, IL-8 and adhesion molecules including ICAM-1, VCAM-1 and E-selectin on endothelial cells, which can increase endothelial inflammatory responses, result in endothelial activation and dysfunction, and induce atherosclerosis development[108, 109]. Superparamagnetic iron oxide nanoparticles change endothelial cell morphology by dramatically increasing intracellular reactive oxygen species concentrations[110]. These results suggest that some metal nanoparticles could potentially enhance endothelial inflammation and atherosclerosis.

Angiogenesis

Neovascularization is a key feature of atherosclerosis development[111]. New microvessels developed in vasa vasorum, the adventitial layer, nurture the cells in atherosclerotic lesions, contribute to the lesion progression, and play an important role in lesion destabilization and rupture[111–113]. Integrin is composed of two transmembrane subunits (α and β) via noncovalent bonds, and plays an important role in interaction of cell to cell, and cell to extracellular matrix[114]. The $\alpha_v\beta_3$ integrin is widely expressed by monocytes, endothelial cells, vascular smooth muscle cells, and fibroblasts, and it involves in the regulation of many intracellular signaling pathways to modulate cell migration, recruitment and invasion during angiogenesis[115–117]. The $\alpha_v\beta_3$ integrin is upregulated in those cells, especially endothelial cells, when they are induced by the angiogenic stimuli[112]. Therefore, it becomes a common target for imaging neoangiogenesis (Table 3).

Winter et al. has developed an $\alpha_v\beta_3$ integrin-targeted paramagnetic nanoparticles. After intravenous injection of those nanoparticles to New Zealand White rabbits fed with high cholesterol diet, nanoparticles targeted new angiogenic vessels and detected neoangiogenesis in the early-stage of atherosclerotic lesions[24]. This group later developed theranostic nanoparticles, the previous $\alpha_v\beta_3$ integrin-targeted paramagnetic nanoparticles carrying fumagillin and atorvastatin[118]. Fumagillin can inhibit blood vessel formation[119]. Atorvastatin (Lipitor), a type of statin drugs, can decrease cholesterol biosynthesis via inhibiting the key enzyme, 3-hydroxy-3-methyl-glutaryl-CoA reductase (HMG-CoA reductase)[120]. The theranostic nanoparticles allowed them to treat and visualize the improvement of atherosclerosis simultaneously. After the nanoparticles was administered to hyperlipidemic rabbits, the $\alpha_v\beta_3$ integrin-targeted fumagillin nanoparticles significantly decreased the neovascular signals by more than 50%, while the $\alpha_v\beta_3$ integrin-targeted fumagillin and atorvastatin nanoparticles exhibited higher and sustainable antianogenic effects[118]. The $\alpha_v\beta_3$ integrin-targeted nanoparticles can also be used for evaluating anti-angiogenic therapeutic responses in patients with the peripheral vascular disease[43].

Proteolysis, Apoptosis and Thrombosis

Proteases, mainly capsineses and matrix metalloproteinases (MMPs), are excreted from intimal macrophages and foam cells[121]. Increased expression of MMPs is associated with decreased thickness of the fibrous cap and increased lesion vulnerability. MMPs expression is induced by inflammatory factors, such as IL-1β and TNF-α. Hence, it is a functional marker of active inflammation and lesion vulnerability in atherosclerotic lesions[6]. Schellenberger E et al. synthesized a protease-specific iron oxide nanosensor that can berapidly switched to a high-relaxivity aggregated particle from a stable low-relaxivity stealth state after cleaved by proteases like MMP9[122]. The nanoparticles detected MMP9 activity *in vitro*. Nahrendorf M et al. synthesized protease-specific polymeric nanosensors, and these polymers were cleavable by proteases[123]. After administering them to apoE−/− mice, they imaged the mice using combined fluorescence molecular tomography (FMT) and CT. Results indicated that these nanoparticles imaged protease activity in the atherosclerotic lesions, and robustly detected the therapeutic effects of the anti-inflammatory drug[123] (Table 4).

Foam cells can die from apoptosis, a programmed cell death. Phosphatidylserine is located in the inner leaflet of the cell membrane in normal and healthy cells, but it is translocated to the outer leaflet of the cell membrane in apoptotic cells[124]. It has been used as a target to detect apoptotic cells in atherosclerotic lesions. Annexin A5 (Annexin V) is a 36 kDa protein with high binding affinity to phosphatidylserine[125]. Technetium-99m–labeled annexin A5 successfully detected apoptotic cells in atherosclerotic lesions in 11 human subjects using SPECT, and this modality may open the door to the detection of lesion vulnerability and to identify high risk patients[126]. Superparmagnetic iron oxide particles (SPIONs) conjugated with annexin A5 targeted to apoptotic foamy macrophages in atherosclerotic lesions of Watanabe heritable hyperlipidemic rabbits, and their target specificity was much higher than non-targeted SPIONs[127]. Annexin A5-conjugated micelles also targeted to apoptotic cells in atherosclerotic lesions of apoE−/− mice, and the targeted micelles had more than 100-fold dose advantage than non-targeted micelles[128]. Apoptotic cells have mitochondrial membrane potential collapse. In another study, synthetic HDL nanoparticles carrying quantum dots were decorated with apoA1 and triphenylphosphonium (TPP) cations, which were used for detecting mitochondrial membrane potential collapse and identifying apoptotic cells [129].

Thrombus formation and its subsequent blockage of blood circulation cause most of myocardial infarction or stroke. Thrombosis is the formation of a blood clot after activation of platelets and the clotting cascade[130]. Fibrin, platelets, erythrocytes, and leukocytes are major components of thrombi[130]. Many fibrin-targeted nanoparticles have been developed to detect thrombi by modifying the surface of nanoparticles with fibrin antibodies or binding peptides[21, 131–134]. Peter D et al. loaded anticoagulant drug hirulog into the fibrin-targeted micelles. The targeted micelles increased hirulog concentrations in the rupture-prone lesion areas and significantly decreased thrombin activity in the lesions[133]. Platelet-targeted nanoparticles were also developed by conjugating platelet antibodies on their surface, which may have a potential to inhibit thrombus formation via decreasing platelet activities[135, 136].

LIPID LOWERING AND ANTI-INFLAMMATORY THERAPY

Lipoprotein-mediated Treatment

LDL, the cholesterol-rich lipoproteins, are derived from very low-density lipoproteins (VLDL). VLDL are triglyceride-rich lipoproteins. Triglyceride in VLDL is hydrolyzed by lipases and removed, making VLDL to turn into intermediate-density lipoproteins (IDL), which are in turn converted to LDL after triglyceride hydrolysis and removal. LDL can deposit cholesterol to peripheral tissues including the blood vessel wall. LDL can be taken up by the liver via binding to LDL receptor and LDL receptor-related protein (LRP) completing a process called the endogenous pathway of lipoprotein transport. ApoB100 is a signature apolipoprotein on VLDL, IDL and LDL, and is required for assembling VLDL in the liver. Decreasing apoB100 expression in the liver can reduce VLDL production, further decrease circulating LDL particle concentrations. ApoB-specific siRNA has been encapsulated into liposomes[137]. After intravenous administration of those liposomes into cynomolgus monkeys, they found significantly decreased liver apoB gene expression, lower serum concentrations of apoB100, total cholesterol and LDL-cholesterol in those non-human

primates. Proprotein convertase subtilisin/kexin type 9 (PCSK9) is a secretory serine protease, and this enzyme can bind to LDL receptor to prevent it from being recycled back to the cell surface, and thus enhancing LDL receptor destruction in the cells, especially hepatocytes[138]. Decreased liver LDL receptor levels are associated with increased circulating LDL-cholesterol concentrations. Mutation or decreased expression of PCSK9 correlates with lowered circulating LDL-cholesterol concentrations, and has vascular benefits[139]. Intravenous administration of the PCSK9 siRNA-loaded nanoparticles into different animal models including mouse, rat, non-human primate decreased levels of PCSK9 transcripts in the liver[140]. These nanoparticles also lowered plasma concentrations of PCSK9 protein and LDL-cholesterol, but had little effect on plasma concentrations of HDL-cholesterol and triglyceride[140].

HDL pick up cholesterol from intimal macrophages and other peripheral cells, and send it back to the liver for cholesterol elimination completing a process termed reverse cholesterol transport[141, 142]. ApoA1 is a signature apolipoprotein on HDL. Increased circulating HDL or apoA1 concentrations correlate with decreased risks of developing atherosclerosis[143]. Many rHDL or HDL-mimic nanoparticles are developed by using lipids and apoA-1 or its derived peptides[144] (Table 5). $ApoA1_{milano}$, a molecular variant of apoA-1, has many cardiovascular benefits including anti-atherogenic, anti-thrombotic, anti-platelet effects. Kaul S et al. made reconstituted HDL nanoparticles (rHDL) using $ApoA1_{milano}$ and phospholipid complex[145]. After intravenous administration of those nanoparticles into apoE −/− mice, the aortic cholesterol content was decreased, and the function of endothelial cells was improved[145]. Luthi AJ et al. made a functional mimic of HDL (fmHDL) using a gold nanoparticle coating with a phospholipid bilayer and apoA-I[146]. They demonstrated that fmHDL accepted cholesterol from macrophages via ABCA1, ABCG1 and SR-B1[146]. Direct administration of rHDL can increase reverse cholesterol transport and subsequently decrease atherosclerosis risk[147]. Shaw JA et al. found that infusion of rHDL increased reverse cholesterol transport capacity, decreased macrophage number and lipid content in lesions, and reduced lesion volume in humans[148]. Duivenvoorden R et al. intravenously administered statin-loaded rHDL to apoE−/− mice and found that these nanoparticles delivered statin to the atherosclerotic lesions, decreased macrophage content in the lesions, lowered lesion inflammatory response. One-week of high dose treatment significantly decreased inflammation in advanced lesions, while three-month low dose treatment inhibited lesion inflammation progression[149].

Anti-inflammatory Treatment

Atherosclerosis is a lipid-driven slowly progressing chronic inflammatory disorder of the arteries[150]. Treatment of atherosclerosis is still mainly focused on lowering blood lipid concentrations, which partially reduces the risk for cardiovascular disease[151, 152]. To further improve treatment of patients, targeting of inflammatory pathways is now believed to offer an additional benefit[153]. Dexamethasone (DXM), an anti-inflammatory steroid drug, can inhibit atherosclerosis development via decreasing intimal macrophage recruitment and foam cell formation[154, 155]. However, long-term administration of DXM has side effects including hypertension, weight gain and depression[156]. Chono S et al made DXM-loaded liposomes with different particle sizes (70, 200 and 500 nm), and intravenously administered

them into atherogenic mice[156]. As compared to free DXM and liposomes with other sizes, L200 (DXM-loaded liposomes with the size of 200 nm in diameter) significantly decreased aortic cholesterol content, which correlated with increased aortic uptake of DXM. L200 had a potent dose advantage as indicated by higher anti-atherogenic effects at 55 μg/kg body weight than free DXM at 550 μg/kg body weight[156]. Glucocorticoid is a potent anti-inflammatory steroid drug, and has been studied for atherosclerosis treatment[157]. Due to its side effects and poor pharmacokinetic profile, glucocorticoid has not been used for atherosclerosis treatment in the clinic[158]. After giving a single intravenous administration of glucocorticoid-loaded liposomes at dose of 15 mg/kg into a rabbits model with atherosclerosis, Lobatto ME found a significant decrease in inflammatory response at day 2, and this inhibitory effect lasted for additional 5 days[157]. Importantly, the lowered inflammation correlated with decreased intimal macrophage content in the animals[157]. This group also developed a good manufacturing practice (GMP)-grade prednisolone phosphate (PLP)-loaded liposomes (L-PLP)[159]. Data from pharmacokinetics and toxicokinetics studies indicated that these liposomes had longer circulation half-life and less side effects than free PLP in rats[159]. Intravenous administration of these liposomes into hyperlipidemic New Zealand white rabbits decreased the inflammatory response in the artery wall[159]. Van der Valk FM et al. intravenously administered L-PLP to patients with iliofemoral atherosclerosis[160]. Compared to free PLP, L-PLP increased the drug's half-life by 7- to 15-fold, which was partially contributed to its increased accumulation in atherosclerotic lesion macrophages[160]. Although the long-circulating L-PLP have been successfully delivered to lesion macrophages, they did not decrease inflammatory responses in the artery walls of patients, who had atherosclerotic CVD[160]. The inconsistency between animal studies and the human trial could be due to insufficient dose of L-PLP, or a short treatment duration in the human trial[157, 159, 160]. Additionally, their effects on host defense in acute inflammatory situations are yet to be investigated[161].

CONCLUDING REMARKS

Atherosclerosis is a silent, progressive disease, and it cannot be easily detected by the current imaging methods at its early stage. Current therapeutic approaches treat atherosclerosis systemically, not locally, which is often associated with decreased efficacy and increased side effects. Nanoparticle-mediated, targeted delivery of diagnostic agents or therapeutic compounds to specific molecules, cells, or tissues represents an innovative approach for the diagnosis and treatment of atherosclerosis. Nanoencapsulation in combination with targeted delivery may enhance stability and bioavailability of agents and drugs, improve their pharmacokinetics, increase detection sensitivity and therapeutic efficacy, and decrease unintended effects directed to the normal tissues. However, it should be pointed that the efficacy of nanoparticles is largely proved in the *in vitro* and animal model studies, and their movement to clinical phases still faces substantial challenges. Future studies are expected to not only address the translational value, but also further elucidate the working modes for more specifically targeted application. Another emerging direction is to develop multifunctional nanoparticles allowing multimodal imaging and targeted delivery of the therapeutic compounds, which are expected to have broader clinical application. Despite being still in the early stage, the steady progress has been made in both

basic research and application study in the field, which makes the diagnostic and therapeutic values of nanoparticle technology in atherosclerosis increasingly promising. We are optimistic in anticipating more breakthroughs to come along in a near future.

Acknowledgments

The work was supported by Grant Number R15AT007013 and 1R15AT008733-01 from the National Center for Complementary and Integrative Health. The content is solely the responsibility of the authors and does not necessarily represent the official views of the National Center for Complementary and Integrative Health or the National Institutes of Health. Additional support was provided by the Burleson's Family Foundation and College of Human Sciences at Texas Tech University, Lubbock, TX.

References

1. Quillard, T.; Croce, KJ. Cardiovascular Imaging. Springer; 2015. Pathobiology and Mechanisms of Atherosclerosis; p. 3-38.
2. Moore KJ, Sheedy FJ, Fisher EA. Macrophages in atherosclerosis: a dynamic balance. Nat Rev Immunol. 2013; 13:709–721. [PubMed: 23995626]
3. Swift MR, Weinstein BM. Arterial-venous specification during development. Circulation research. 2009; 104:576–588. [PubMed: 19286613]
4. Libby P. Inflammation in atherosclerosis. Arteriosclerosis, thrombosis, and vascular biology. 2012; 32:2045–2051.
5. Pober JS, Sessa WC. Evolving functions of endothelial cells in inflammation. Nature Reviews Immunology. 2007; 7:803–815.
6. Libby P. Inflammation in atherosclerosis. Nature. 2002; 420:868–874. [PubMed: 12490960]
7. Matsui M, Homma H. Biochemistry and molecular biology of drug-metabolizing sulfotransferase. Int J Biochem. 1994; 26:1237–1247. [PubMed: 7851628]
8. Libby P, Ridker PM. Inflammation and atherosclerosis: role of C-reactive protein in risk assessment. Am J Med. 2004; 116(Suppl 6A):9S–16S. [PubMed: 15050187]
9. Libby P, Sasiela W. Plaque stabilization: Can we turn theory into evidence? Am J Cardiol. 2006; 98:26P–33P.
10. Jaffer FA, Libby P, Weissleder R. Optical and multimodality molecular imaging: insights into atherosclerosis. Arterioscler Thromb Vasc Biol. 2009; 29:1017–1024. [PubMed: 19359659]
11. Libby P, DiCarli M, Weissleder R. The vascular biology of atherosclerosis and imaging targets. J Nucl Med. 2010; 51(Suppl 1):33S–37S. [PubMed: 20395349]
12. Arbab-Zadeh A, Nakano M, Virmani R, Fuster V. Acute coronary events. Circulation. 2012; 125:1147–1156. [PubMed: 22392862]
13. Naghavi M, Libby P, Falk E, Casscells SW, Litovsky S, Rumberger J, Badimon JJ, Stefanadis C, Moreno P, Pasterkamp G, et al. From vulnerable plaque to vulnerable patient: a call for new definitions and risk assessment strategies: Part I. Circulation. 2003; 108:1664–1672. [PubMed: 14530185]
14. Iwata H, Aikawa M. Liver-artery interactions via the plasminogen-CD36 axis in macrophage foam cell formation: new evidence for the role of remote organ crosstalk in atherosclerosis. Circulation. 2013; 127:1173–1176. [PubMed: 23509031]
15. Robbins CS, Hilgendorf I, Weber GF, Theurl I, Iwamoto Y, Figueiredo J-L, Gorbatov R, Sukhova GK, Gerhardt LM, Smyth D. Local proliferation dominates lesional macrophage accumulation in atherosclerosis. Nature medicine. 2013; 19:1166–1172.
16. Quillard T, Croce K, Jaffer FA, Weissleder R, Libby P. Molecular imaging of macrophage protease activity in cardiovascular inflammation in vivo. Thromb Haemost. 2011; 105:828–836. [PubMed: 21225096]
17. Lobatto ME, Fuster V, Fayad ZA, Mulder WJ. Perspectives and opportunities for nanomedicine in the management of atherosclerosis. Nat Rev Drug Discov. 2011; 10:835–852. [PubMed: 22015921]

18. Patel SK, Janjic JM. Macrophage Targeted Theranostics as Personalized Nanomedicine Strategies for Inflammatory Diseases. Theranostics. 2015; 5:150. [PubMed: 25553105]
19. Peer D, Karp JM, Hong S, Farokhzad OC, Margalit R, Langer R. Nanocarriers as an emerging platform for cancer therapy. Nat Nanotechnol. 2007; 2:751–760. [PubMed: 18654426]
20. Yu X, Song SK, Chen J, Scott MJ, Fuhrhop RJ, Hall CS, Gaffney PJ, Wickline SA, Lanza GM. High-resolution MRI characterization of human thrombus using a novel fibrin-targeted paramagnetic nanoparticle contrast agent. Magn Reson Med. 2000; 44:867–872. [PubMed: 11108623]
21. Flacke S, Fischer S, Scott MJ, Fuhrhop RJ, Allen JS, McLean M, Winter P, Sicard GA, Gaffney PJ, Wickline SA, et al. Novel MRI contrast agent for molecular imaging of fibrin: implications for detecting vulnerable plaques. Circulation. 2001; 104:1280–1285. [PubMed: 11551880]
22. Ruehm SG, Corot C, Vogt P, Kolb S, Debatin JF. Magnetic resonance imaging of atherosclerotic plaque with ultrasmall superparamagnetic particles of iron oxide in hyperlipidemic rabbits. Circulation. 2001; 103:415–422. [PubMed: 11157694]
23. Kang HW, Josephson L, Petrovsky A, Weissleder R, Bogdanov A Jr. Magnetic resonance imaging of inducible E-selectin expression in human endothelial cell culture. Bioconjug Chem. 2002; 13:122–127. [PubMed: 11792187]
24. Winter PM, Morawski AM, Caruthers SD, Fuhrhop RW, Zhang H, Williams TA, Allen JS, Lacy EK, Robertson JD, Lanza GM, et al. Molecular imaging of angiogenesis in early-stage atherosclerosis with alpha(v)beta3-integrin-targeted nanoparticles. Circulation. 2003; 108:2270–2274. [PubMed: 14557370]
25. Ye K, Qin J, Peng Z, Yang X, Huang L, Yuan F, Peng C, Jiang M, Lu X. Polyethylene glycol-modified dendrimer-entrapped gold nanoparticles enhance CT imaging of blood pool in atherosclerotic mice. Nanoscale research letters. 2014; 9:1–12. [PubMed: 24380376]
26. Qin J, Peng C, Zhao B, Ye K, Yuan F, Peng Z, Yang X, Huang L, Jiang M, Zhao Q. Noninvasive detection of macrophages in atherosclerotic lesions by computed tomography enhanced with PEGylated gold nanoparticles. International journal of nanomedicine. 2014; 9:5575. [PubMed: 25506213]
27. Nie S, Zhang J, Martinez-Zaguilan R, Sennoune S, Hossen MN, Wang S. Detecting Atherosclerotic Lesions and Intimal Macrophages Using Targeted Nanovesicles. Controlled Release.
28. Tang TY, Howarth SP, Miller SR, Graves MJ, Patterson AJ, JM UK-I, Li ZY, Walsh SR, Brown AP, Kirkpatrick PJ, et al. The ATHEROMA (Atorvastatin Therapy: Effects on Reduction of Macrophage Activity) Study. Evaluation using ultrasmall superparamagnetic iron oxide-enhanced magnetic resonance imaging in carotid disease. J Am Coll Cardiol. 2009; 53:2039–2050. [PubMed: 19477353]
29. Kooi ME, Cappendijk VC, Cleutjens KB, Kessels AG, Kitslaar PJ, Borgers M, Frederik PM, Daemen MJ, van Engelshoven JM. Accumulation of ultrasmall superparamagnetic particles of iron oxide in human atherosclerotic plaques can be detected by in vivo magnetic resonance imaging. Circulation. 2003; 107:2453–2458. [PubMed: 12719280]
30. Koga, J-i; Aikawa, M. Cardiovascular Imaging. Springer; 2015. Molecular Imaging of Macrophages in Atherosclerosis; p. 65-78.
31. Leuschner F, Nahrendorf M. Molecular Imaging of coronary atherosclerosis and myocardial infarction considerations for the bench and perspectives for the clinic. Circulation research. 2011; 108:593–606. [PubMed: 21372291]
32. Weissleder R, Nahrendorf M, Pittet MJ. Imaging macrophages with nanoparticles. Nature materials. 2014; 13:125–138. [PubMed: 24452356]
33. Murray PJ, Wynn TA. Protective and pathogenic functions of macrophage subsets. Nature reviews immunology. 2011; 11:723–737.
34. Karagkiozaki V, Logothetidis S, Pappa AM. Nanomedicine for Atherosclerosis: Molecular Imaging and Treatment. J Biomed Nanotechnol. 2015; 11:191–210. [PubMed: 26349296]
35. Torchilin VP. Multifunctional nanocarriers. Adv Drug Deliv Rev. 2006; 58:1532–1555. [PubMed: 17092599]
36. Wen S, Liu D-F, Cui Y, Harris SS, Chen Y-c, Li KC, Ju S-h, Teng G-J. In vivo MRI detection of carotid atherosclerotic lesions and kidney inflammation in ApoE-deficient mice by using LOX-1

targeted iron nanoparticles. Nanomedicine: Nanotechnology, Biology and Medicine. 2014; 10:639–649.

37. Mulder WJ, Strijkers GJ, Briley-Saboe KC, Frias JC, Aguinaldo JGS, Vucic E, Amirbekian V, Tang C, Chin PT, Nicolay K. Molecular imaging of macrophages in atherosclerotic plaques using bimodal PEG-micelles. Magnetic resonance in medicine. 2007; 58:1164–1170. [PubMed: 18046703]
38. Michalska M, Machtoub L, Manthey HD, Bauer E, Herold V, Krohne G, Lykowsky G, Hildenbrand M, Kampf T, Jakob P, et al. Visualization of vascular inflammation in the atherosclerotic mouse by ultrasmall superparamagnetic iron oxide vascular cell adhesion molecule-1-specific nanoparticles. Arterioscler Thromb Vasc Biol. 2012; 32:2350–2357. [PubMed: 22879583]
39. Chacko AM, Hood ED, Zern BJ, Muzykantov VR. Targeted Nanocarriers for Imaging and Therapy of Vascular Inflammation. Curr Opin Colloid Interface Sci. 2011; 16:215–227. [PubMed: 21709761]
40. Briley-Saebo KC, Cho YS, Shaw PX, Ryu SK, Mani V, Dickson S, Izadmehr E, Green S, Fayad ZA, Tsimikas S. Targeted iron oxide particles for in vivo magnetic resonance detection of atherosclerotic lesions with antibodies directed to oxidation-specific epitopes. Journal of the American College of Cardiology. 2011; 57:337–347. [PubMed: 21106318]
41. Briley-Saebo KC, Shaw PX, Mulder WJ, Choi S-H, Vucic E, Aguinaldo JGS, Witztum JL, Fuster V, Tsimikas S, Fayad ZA. Targeted molecular probes for imaging atherosclerotic lesions with magnetic resonance using antibodies that recognize oxidation-specific epitopes. Circulation. 2008; 117:3206–3215. [PubMed: 18541740]
42. Klegerman ME, Zou Y, McPherson DD. Fibrin targeting of echogenic liposomes with inactivated tissue plasminogen activator. J Liposome Res. 2008; 18:95–112. [PubMed: 18569446]
43. Winter PM, Caruthers SD, Allen JS, Cai K, Williams TA, Lanza GM, Wickline SA. Molecular imaging of angiogenic therapy in peripheral vascular disease with alphanubeta3-integrin-targeted nanoparticles. Magn Reson Med. 2010; 64:369–376. [PubMed: 20665780]
44. Sadat U, Jaffer FA, van Zandvoort MA, Nicholls SJ, Ribatti D, Gillard JH. Inflammation and neovascularization intertwined in atherosclerosis: imaging of structural and molecular imaging targets. Circulation. 2014; 130:786–794. [PubMed: 25156914]
45. Sima AV, Stancu CS, Simionescu M. Vascular endothelium in atherosclerosis. Cell Tissue Res. 2009; 335:191–203. [PubMed: 18797930]
46. Kim Y, Lobatto ME, Kawahara T, Lee Chung B, Mieszawska AJ, Sanchez-Gaytan BL, Fay F, Senders ML, Calcagno C, Becraft J, et al. Probing nanoparticle translocation across the permeable endothelium in experimental atherosclerosis. Proc Natl Acad Sci U S A. 2014; 111:1078–1083. [PubMed: 24395808]
47. Quillard T, Libby P. Molecular imaging of atherosclerosis for improving diagnostic and therapeutic development. Circ Res. 2012; 111:231–244. [PubMed: 22773426]
48. Stoneman V, Braganza D, Figg N, Mercer J, Lang R, Goddard M, Bennett M. Monocyte/macrophage suppression in CD11b diphtheria toxin receptor transgenic mice differentially affects atherogenesis and established plaques. Circ Res. 2007; 100:884–893. [PubMed: 17322176]
49. Weber C, Zernecke A, Libby P. The multifaceted contributions of leukocyte subsets to atherosclerosis: lessons from mouse models. Nat Rev Immunol. 2008; 8:802–815. [PubMed: 18825131]
50. Packard RR, Lichtman AH, Libby P. Innate and adaptive immunity in atherosclerosis. Semin Immunopathol. 2009; 31:5–22. [PubMed: 19449008]
51. Boyer C, Whittaker MR, Bulmus V, Liu J, Davis TP. The design and utility of polymer-stabilized iron-oxide nanoparticles for nanomedicine applications. NPG Asia Materials. 2010; 2:23–30.
52. Harel-Adar T, Mordechai TB, Amsalem Y, Feinberg MS, Leor J, Cohen S. Modulation of cardiac macrophages by phosphatidylserine-presenting liposomes improves infarct repair. Proceedings of the National Academy of Sciences. 2011; 108:1827–1832.
53. Park YM. CD36, a scavenger receptor implicated in atherosclerosis. Exp Mol Med. 2014; 46:e99. [PubMed: 24903227]

54. Calvo D, Dopazo J, Vega MA. The CD36, CLA-1 (CD36L1), and LIMPII (CD36L2) gene family: cellular distribution, chromosomal location, and genetic evolution. Genomics. 1995; 25:100–106. [PubMed: 7539776]
55. Febbraio M, Abumrad NA, Hajjar DP, Sharma K, Cheng W, Pearce SF, Silverstein RL. A null mutation in murine CD36 reveals an important role in fatty acid and lipoprotein metabolism. J Biol Chem. 1999; 274:19055–19062. [PubMed: 10383407]
56. Febbraio M, Podrez EA, Smith JD, Hajjar DP, Hazen SL, Hoff HF, Sharma K, Silverstein RL. Targeted disruption of the class B scavenger receptor CD36 protects against atherosclerotic lesion development in mice. J Clin Invest. 2000; 105:1049–1056. [PubMed: 10772649]
57. Moore KJ, Freeman MW. Scavenger receptors in atherosclerosis: beyond lipid uptake. Arterioscler Thromb Vasc Biol. 2006; 26:1702–1711. [PubMed: 16728653]
58. Febbraio M, Guy E, Silverstein RL. Stem cell transplantation reveals that absence of macrophage CD36 is protective against atherosclerosis. Arterioscler Thromb Vasc Biol. 2004; 24:2333–2338. [PubMed: 15486305]
59. Marleau S, Harb D, Bujold K, Avallone R, Iken K, Wang Y, Demers A, Sirois MG, Febbraio M, Silverstein RL, et al. EP 80317, a ligand of the CD36 scavenger receptor, protects apolipoprotein E-deficient mice from developing atherosclerotic lesions. FASEB J. 2005; 19:1869–1871. [PubMed: 16123174]
60. Curtiss LK. Reversing atherosclerosis? N Engl J Med. 2009; 360:1144–1146. [PubMed: 19279347]
61. Terpstra V, Bird DA, Steinberg D. Evidence that the lipid moiety of oxidized low density lipoprotein plays a role in its interaction with macrophage receptors. Proc Natl Acad Sci U S A. 1998; 95:1806–1811. [PubMed: 9465098]
62. Bird DA, Gillotte KL, Horkko S, Friedman P, Dennis EA, Witztum JL, Steinberg D. Receptors for oxidized low-density lipoprotein on elicited mouse peritoneal macrophages can recognize both the modified lipid moieties and the modified protein moieties: implications with respect to macrophage recognition of apoptotic cells. Proc Natl Acad Sci U S A. 1999; 96:6347–6352. [PubMed: 10339590]
63. Podrez EA, Poliakov E, Shen Z, Zhang R, Deng Y, Sun M, Finton PJ, Shan L, Febbraio M, Hajjar DP, et al. A novel family of atherogenic oxidized phospholipids promotes macrophage foam cell formation via the scavenger receptor CD36 and is enriched in atherosclerotic lesions. J Biol Chem. 2002; 277:38517–38523. [PubMed: 12145296]
64. Podrez EA, Poliakov E, Shen Z, Zhang R, Deng Y, Sun M, Finton PJ, Shan L, Gugiu B, Fox PL, et al. Identification of a novel family of oxidized phospholipids that serve as ligands for the macrophage scavenger receptor CD36. J Biol Chem. 2002; 277:38503–38516. [PubMed: 12105195]
65. Greenberg ME, Li XM, Gugiu BG, Gu X, Qin J, Salomon RG, Hazen SL. The lipid whisker model of the structure of oxidized cell membranes. J Biol Chem. 2008; 283:2385–2396. [PubMed: 18045864]
66. Kar NS, Ashraf MZ, Valiyaveettil M, Podrez EA. Mapping and characterization of the binding site for specific oxidized phospholipids and oxidized low density lipoprotein of scavenger receptor CD36. J Biol Chem. 2008; 283:8765–8771. [PubMed: 18245080]
67. Collot-Teixeira S, Martin J, McDermott-Roe C, Poston R, McGregor JL. CD36 and macrophages in atherosclerosis. Cardiovasc Res. 2007; 75:468–477. [PubMed: 17442283]
68. Lipinski MJ, Frias JC, Amirbekian V, Briley-Saebo KC, Mani V, Samber D, Abbate A, Aguinaldo JG, Massey D, Fuster V, et al. Macrophage-specific lipid-based nanoparticles improve cardiac magnetic resonance detection and characterization of human atherosclerosis. JACC Cardiovasc Imaging. 2009; 2:637–647. [PubMed: 19442953]
69. de Winther MP, van Dijk KW, Havekes LM, Hofker MH. Macrophage scavenger receptor class A: A multifunctional receptor in atherosclerosis. Arterioscler Thromb Vasc Biol. 2000; 20:290–297. [PubMed: 10669623]
70. Segers FM, den Adel B, Bot I, van der Graaf LM, van der Veer EP, Gonzalez W, Raynal I, de Winther M, Wodzig WK, Poelmann RE. Scavenger Receptor-AI-Targeted Iron Oxide Nanoparticles for In Vivo MRI Detection of Atherosclerotic Lesions. Arteriosclerosis, thrombosis, and vascular biology. 2013; 33:1812–1819.

71. Amirbekian V, Lipinski MJ, Briley-Saebo KC, Amirbekian S, Aguinaldo JGS, Weinreb DB, Vucic E, Frias JC, Hyafil F, Mani V. Detecting and assessing macrophages in vivo to evaluate atherosclerosis noninvasively using molecular MRI. Proceedings of the National Academy of Sciences. 2007; 104:961–966.
72. Duivenvoorden R, Tang J, Cormode DP, Mieszawska AJ, Izquierdo-Garcia D, Ozcan C, Otten MJ, Zaidi N, Lobatto ME, van Rijs SM, et al. A statin-loaded reconstituted high-density lipoprotein nanoparticle inhibits atherosclerotic plaque inflammation. Nat Commun. 2014; 5:3065. [PubMed: 24445279]
73. Leuschner F, Dutta P, Gorbatov R, Novobrantseva TI, Donahoe JS, Courties G, Lee KM, Kim JI, Markmann JF, Marinelli B. Therapeutic siRNA silencing in inflammatory monocytes in mice. Nature biotechnology. 2011; 29:1005–1010.
74. Martinez FO, Gordon S. The M1 and M2 paradigm of macrophage activation: time for reassessment. F1000Prime Rep. 2014; 6:13. [PubMed: 24669294]
75. Italiani P, Boraschi D. From Monocytes to M1/M2 Macrophages: Phenotypical vs. Functional Differentiation. Front Immunol. 2014; 5:514. [PubMed: 25368618]
76. Swirski FK, Libby P, Aikawa E, Alcaide P, Luscinskas FW, Weissleder R, Pittet MJ. Ly-6Chi monocytes dominate hypercholesterolemia-associated monocytosis and give rise to macrophages in atheromata. J Clin Invest. 2007; 117:195–205. [PubMed: 17200719]
77. Majmudar MD, Yoo J, Keliher EJ, Truelove JJ, Iwamoto Y, Sena B, Dutta P, Borodovsky A, Fitzgerald K, Di Carli MF. Polymeric nanoparticle PET/MR imaging allows macrophage detection in atherosclerotic plaques. Circulation research. 2013; 112:755–761. [PubMed: 23300273]
78. McCarthy JR, Korngold E, Weissleder R, Jaffer FA. A light-activated theranostic nanoagent for targeted macrophage ablation in inflammatory atherosclerosis. Small. 2010; 6:2041–2049. [PubMed: 20721949]
79. Wang S, Wu D, Matthan NR, Lamon-Fava S, Lecker JL, Lichtenstein AH. Reduction in dietary omega-6 polyunsaturated fatty acids: eicosapentaenoic acid plus docosahexaenoic acid ratio minimizes atherosclerotic lesion formation and inflammatory response in the LDL receptor null mouse. Atherosclerosis. 2009; 204:147–155. [PubMed: 18842266]
80. Im SS, Osborne TF. Liver x receptors in atherosclerosis and inflammation. Circ Res. 2011; 108:996–1001. [PubMed: 21493922]
81. Calkin AC, Tontonoz P. Liver x receptor signaling pathways and atherosclerosis. Arterioscler Thromb Vasc Biol. 2010; 30:1513–1518. [PubMed: 20631351]
82. Bradley MN, Hong C, Chen M, Joseph SB, Wilpitz DC, Wang X, Lusis AJ, Collins A, Hseuh WA, Collins JL, et al. Ligand activation of LXR beta reverses atherosclerosis and cellular cholesterol overload in mice lacking LXR alpha and apoE. J Clin Invest. 2007; 117:2337–2346. [PubMed: 17657314]
83. Rosenson RS, Brewer HB Jr, Davidson WS, Fayad ZA, Fuster V, Goldstein J, Hellerstein M, Jiang XC, Phillips MC, Rader DJ, et al. Cholesterol efflux and atheroprotection: advancing the concept of reverse cholesterol transport. Circulation. 2012; 125:1905–1919. [PubMed: 22508840]
84. Joseph SB, Castrillo A, Laffitte BA, Mangelsdorf DJ, Tontonoz P. Reciprocal regulation of inflammation and lipid metabolism by liver X receptors. Nat Med. 2003; 9:213–219. [PubMed: 12524534]
85. Vedhachalam C, Liu L, Nickel M, Dhanasekaran P, Anantharamaiah GM, Lund-Katz S, Rothblat GH, Phillips MC. Influence of ApoA-I structure on the ABCA1-mediated efflux of cellular lipids. J Biol Chem. 2004; 279:49931–49939. [PubMed: 15383537]
86. Baranova I, Vishnyakova T, Bocharov A, Chen Z, Remaley AT, Stonik J, Eggerman TL, Patterson AP. Lipopolysaccharide down regulates both scavenger receptor B1 and ATP binding cassette transporter A1 in RAW cells. Infect Immun. 2002; 70:2995–3003. [PubMed: 12010990]
87. Asztalos BF, Schaefer EJ, Horvath KV, Yamashita S, Miller M, Franceschini G, Calabresi L. Role of LCAT in HDL remodeling: investigation of LCAT deficiency states. J Lipid Res. 2007; 48:592–599. [PubMed: 17183024]
88. Rosenson RS, Brewer HB Jr, Ansell BJ, Barter P, Chapman MJ, Heinecke JW, Kontush A, Tall AR, Webb NR. Dysfunctional HDL and atherosclerotic cardiovascular disease. Nat Rev Cardiol. 2015

89. Iverson NM, Plourde NM, Sparks SM, Wang J, Patel EN, Shah PS, Lewis DR, Zablocki KR, Nackman GB, Uhrich KE. Dual use of amphiphilic macromolecules as cholesterol efflux triggers and inhibitors of macrophage athero-inflammation. Biomaterials. 2011; 32:8319–8327. [PubMed: 21816466]

90. Zhang XQ, Even-Or O, Xu X, van Rosmalen M, Lim L, Gadde S, Farokhzad OC, Fisher EA. Nanoparticles containing a liver X receptor agonist inhibit inflammation and atherosclerosis. Adv Healthc Mater. 2015; 4:228–236. [PubMed: 25156796]

91. Meng J, Yang XD, Jia L, Liang XJ, Wang C. Impacts of nanoparticles on cardiovascular diseases: modulating metabolism and function of endothelial cells. Curr Drug Metab. 2012; 13:1123–1129. [PubMed: 22380015]

92. Agyare E, Kandimalla K. Delivery of Polymeric Nanoparticles to Target Vascular Diseases. J Biomol Res Ther. 2014; 3

93. Chiu JJ, Chien S. Effects of disturbed flow on vascular endothelium: pathophysiological basis and clinical perspectives. Physiol Rev. 2011; 91:327–387. [PubMed: 21248169]

94. Jayagopal A, Linton MF, Fazio S, Haselton FR. Insights into atherosclerosis using nanotechnology. Curr Atheroscler Rep. 2010; 12:209–215. [PubMed: 20425261]

95. Burtea C, Ballet S, Laurent S, Rousseaux O, Dencausse A, Gonzalez W, Port M, Corot C, Vander Elst L, Muller RN. Development of a magnetic resonance imaging protocol for the characterization of atherosclerotic plaque by using vascular cell adhesion molecule-1 and apoptosis-targeted ultrasmall superparamagnetic iron oxide derivatives. Arterioscler Thromb Vasc Biol. 2012; 32:e36–e48. [PubMed: 22516067]

96. Muro S, Muzykantov VR. Targeting of antioxidant and anti-thrombotic drugs to endothelial cell adhesion molecules. Curr Pharm Des. 2005; 11:2383–2401. [PubMed: 16022673]

97. Iiyama K, Hajra L, Iiyama M, Li H, DiChiara M, Medoff BD, Cybulsky MI. Patterns of vascular cell adhesion molecule-1 and intercellular adhesion molecule-1 expression in rabbit and mouse atherosclerotic lesions and at sites predisposed to lesion formation. Circ Res. 1999; 85:199–207. [PubMed: 10417402]

98. Cybulsky MI, Iiyama K, Li H, Zhu S, Chen M, Iiyama M, Davis V, Gutierrez-Ramos JC, Connelly PW, Milstone DS. A major role for VCAM-1, but not ICAM-1, in early atherosclerosis. J Clin Invest. 2001; 107:1255–1262. [PubMed: 11375415]

99. Tsourkas A, Shinde-Patil VR, Kelly KA, Patel P, Wolley A, Allport JR, Weissleder R. In vivo imaging of activated endothelium using an anti-VCAM-1 magnetooptical probe. Bioconjug Chem. 2005; 16:576–581. [PubMed: 15898724]

100. Kelly KA, Allport JR, Tsourkas A, Shinde-Patil VR, Josephson L, Weissleder R. Detection of vascular adhesion molecule-1 expression using a novel multimodal nanoparticle. Circ Res. 2005; 96:327–336. [PubMed: 15653572]

101. Nahrendorf M, Jaffer FA, Kelly KA, Sosnovik DE, Aikawa E, Libby P, Weissleder R. Noninvasive vascular cell adhesion molecule-1 imaging identifies inflammatory activation of cells in atherosclerosis. Circulation. 2006; 114:1504–1511. [PubMed: 17000904]

102. Kelly KA, Nahrendorf M, Yu AM, Reynolds F, Weissleder R. In vivo phage display selection yields atherosclerotic plaque targeted peptides for imaging. Mol Imaging Biol. 2006; 8:201–207. [PubMed: 16791746]

103. Lee GY, Kim JH, Oh GT, Lee BH, Kwon IC, Kim IS. Molecular targeting of atherosclerotic plaques by a stabilin-2-specific peptide ligand. J Control Release. 2011; 155:211–217. [PubMed: 21781994]

104. Park K, Hong HY, Moon HJ, Lee BH, Kim IS, Kwon IC, Rhee K. A new atherosclerotic lesion probe based on hydrophobically modified chitosan nanoparticles functionalized by the atherosclerotic plaque targeted peptides. J Control Release. 2008; 128:217–223. [PubMed: 18457896]

105. Alinovi R, Goldoni M, Pinelli S, Campanini M, Aliatis I, Bersani D, Lottici PP, Iavicoli S, Petyx M, Mozzoni P, et al. Oxidative and pro-inflammatory effects of cobalt and titanium oxide nanoparticles on aortic and venous endothelial cells. Toxicol In Vitro. 2015; 29:426–437. [PubMed: 25526690]

106. Guo C, Xia Y, Niu P, Jiang L, Duan J, Yu Y, Zhou X, Li Y, Sun Z. Silica nanoparticles induce oxidative stress, inflammation, and endothelial dysfunction in vitro via activation of the MAPK/Nrf2 pathway and nuclear factor-kappaB signaling. Int J Nanomedicine. 2015; 10:1463–1477. [PubMed: 25759575]

107. Suzuki Y, Tada-Oikawa S, Ichihara G, Yabata M, Izuoka K, Suzuki M, Sakai K, Ichihara S. Zinc oxide nanoparticles induce migration and adhesion of monocytes to endothelial cells and accelerate foam cell formation. Toxicol Appl Pharmacol. 2014; 278:16–25. [PubMed: 24746987]

108. Zhu MT, Wang B, Wang Y, Yuan L, Wang HJ, Wang M, Ouyang H, Chai ZF, Feng WY, Zhao YL. Endothelial dysfunction and inflammation induced by iron oxide nanoparticle exposure: Risk factors for early atherosclerosis. Toxicol Lett. 2011; 203:162–171. [PubMed: 21439359]

109. Aikawa E, Nahrendorf M, Sosnovik D, Lok VM, Jaffer FA, Aikawa M, Weissleder R. Multimodality molecular imaging identifies proteolytic and osteogenic activities in early aortic valve disease. Circulation. 2007; 115:377–386. [PubMed: 17224478]

110. Buyukhatipoglu K, Clyne AM. Superparamagnetic iron oxide nanoparticles change endothelial cell morphology and mechanics via reactive oxygen species formation. J Biomed Mater Res A. 2011; 96:186–195. [PubMed: 21105167]

111. Moreno PR, Purushothaman KR, Sirol M, Levy AP, Fuster V. Neovascularization in human atherosclerosis. Circulation. 2006; 113:2245–2252. [PubMed: 16684874]

112. Khurana R, Simons M, Martin JF, Zachary IC. Role of angiogenesis in cardiovascular disease: a critical appraisal. Circulation. 2005; 112:1813–1824. [PubMed: 16172288]

113. Di Stefano R, Felice F, Balbarini A. Angiogenesis as risk factor for plaque vulnerability. Curr Pharm Des. 2009; 15:1095–1106. [PubMed: 19355951]

114. Sancey L, Ardisson V, Riou LM, Ahmadi M, Marti-Batlle D, Boturyn D, Dumy P, Fagret D, Ghezzi C, Vuillez JP. In vivo imaging of tumour angiogenesis in mice with the alpha(v)beta (3) integrin-targeted tracer 99mTc-RAFT-RGD. Eur J Nucl Med Mol Imaging. 2007; 34:2037–2047. [PubMed: 17674000]

115. Haubner R, Weber WA, Beer AJ, Vabuliene E, Reim D, Sarbia M, Becker KF, Goebel M, Hein R, Wester HJ, et al. Noninvasive visualization of the activated alphavbeta3 integrin in cancer patients by positron emission tomography and [18F]Galacto-RGD. PLoS Med. 2005; 2:e70. [PubMed: 15783258]

116. Bishop GG, McPherson JA, Sanders JM, Hesselbacher SE, Feldman MJ, McNamara CA, Gimple LW, Powers ER, Mousa SA, Sarembock IJ. Selective alpha(v)beta(3)-receptor blockade reduces macrophage infiltration and restenosis after balloon angioplasty in the atherosclerotic rabbit. Circulation. 2001; 103:1906–1911. [PubMed: 11294811]

117. Sluimer JC, Daemen MJ. Novel concepts in atherogenesis: angiogenesis and hypoxia in atherosclerosis. J Pathol. 2009; 218:7–29. [PubMed: 19309025]

118. Winter PM, Caruthers SD, Zhang H, Williams TA, Wickline SA, Lanza GM. Antiangiogenic synergism of integrin-targeted fumagillin nanoparticles and atorvastatin in atherosclerosis. JACC Cardiovasc Imaging. 2008; 1:624–634. [PubMed: 19356492]

119. Williams GR, Sampson MA, Shutler D, Rogers RE. Does fumagillin control the recently detected invasive parasite Nosema ceranae in western honey bees (Apis mellifera)? J Invertebr Pathol. 2008; 99:342–344. [PubMed: 18550078]

120. Nawrocki JW, Weiss SR, Davidson MH, Sprecher DL, Schwartz SL, Lupien PJ, Jones PH, Haber HE, Black DM. Reduction of LDL cholesterol by 25% to 60% in patients with primary hypercholesterolemia by atorvastatin, a new HMG-CoA reductase inhibitor. Arterioscler Thromb Vasc Biol. 1995; 15:678–682. [PubMed: 7749881]

121. Libby P, Ridker PM, Maseri A. Inflammation and atherosclerosis. Circulation. 2002; 105:1135–1143. [PubMed: 11877368]

122. Schellenberger E, Rudloff F, Warmuth C, Taupitz M, Hamm B, Schnorr J. Protease-specific nanosensors for magnetic resonance imaging. Bioconjug Chem. 2008; 19:2440–2445. [PubMed: 19007261]

123. Nahrendorf M, Waterman P, Thurber G, Groves K, Rajopadhye M, Panizzi P, Marinelli B, Aikawa E, Pittet MJ, Swirski FK, et al. Hybrid in vivo FMT-CT imaging of protease activity in

atherosclerosis with customized nanosensors. Arterioscler Thromb Vasc Biol. 2009; 29:1444–1451. [PubMed: 19608968]

124. Fadok VA, Bratton DL, Frasch SC, Warner ML, Henson PM. The role of phosphatidylserine in recognition of apoptotic cells by phagocytes. Cell Death Differ. 1998; 5:551–562. [PubMed: 10200509]
125. Schellenberger EA, Bogdanov A Jr, Hogemann D, Tait J, Weissleder R, Josephson L. Annexin V-CLIO: a nanoparticle for detecting apoptosis by MRI. Mol Imaging. 2002; 1:102–107. [PubMed: 12920851]
126. Kietselaer BL, Reutelingsperger CP, Heidendal GA, Daemen MJ, Mess WH, Hofstra L, Narula J. Noninvasive detection of plaque instability with use of radiolabeled annexin A5 in patients with carotid-artery atherosclerosis. N Engl J Med. 2004; 350:1472–1473.
127. Smith BR, Heverhagen J, Knopp M, Schmalbrock P, Shapiro J, Shiomi M, Moldovan NI, Ferrari M, Lee SC. Localization to atherosclerotic plaque and biodistribution of biochemically derivatized superparamagnetic iron oxide nanoparticles (SPIONs) contrast particles for magnetic resonance imaging (MRI). Biomed Microdevices. 2007; 9:719–727. [PubMed: 17562181]
128. van Tilborg GA, Vucic E, Strijkers GJ, Cormode DP, Mani V, Skajaa T, Reutelingsperger CP, Fayad ZA, Mulder WJ, Nicolay K. Annexin A5-functionalized bimodal nanoparticles for MRI and fluorescence imaging of atherosclerotic plaques. Bioconjug Chem. 2010; 21:1794–1803. [PubMed: 20804153]
129. Marrache S, Dhar S. Biodegradable synthetic high-density lipoprotein nanoparticles for atherosclerosis. Proceedings of the National Academy of Sciences. 2013; 110:9445–9450.
130. Robbie L, Libby P. Inflammation and atherothrombosis. Ann N Y Acad Sci. 2001; 947:167–179. discussion 179–180. [PubMed: 11795264]
131. Winter PM, Caruthers SD, Yu X, Song SK, Chen J, Miller B, Bulte JW, Robertson JD, Gaffney PJ, Wickline SA, et al. Improved molecular imaging contrast agent for detection of human thrombus. Magn Reson Med. 2003; 50:411–416. [PubMed: 12876719]
132. Sirol M, Fuster V, Badimon JJ, Fallon JT, Moreno PR, Toussaint JF, Fayad ZA. Chronic thrombus detection with in vivo magnetic resonance imaging and a fibrin-targeted contrast agent. Circulation. 2005; 112:1594–1600. [PubMed: 16145001]
133. Peters D, Kastantin M, Kotamraju VR, Karmali PP, Gujraty K, Tirrell M, Ruoslahti E. Targeting atherosclerosis by using modular, multifunctional micelles. Proc Natl Acad Sci U S A. 2009; 106:9815–9819. [PubMed: 19487682]
134. Starmans LW, Burdinski D, Haex NP, Moonen RP, Strijkers GJ, Nicolay K, Grull H. Iron oxide nanoparticle-micelles (ION-micelles) for sensitive (molecular) magnetic particle imaging and magnetic resonance imaging. PLoS One. 2013; 8:e57335. [PubMed: 23437371]
135. Jacobin-Valat MJ, Deramchia K, Mornet S, Hagemeyer CE, Bonetto S, Robert R, Biran M, Massot P, Miraux S, Sanchez S, et al. MRI of inducible P-selectin expression in human activated platelets involved in the early stages of atherosclerosis. NMR Biomed. 2011; 24:413–424. [PubMed: 21192086]
136. Jacobin-Valat MJ, Laroche-Traineau J, Lariviere M, Mornet S, Sanchez S, Biran M, Lebaron C, Boudon J, Lacomme S, Cerutti M, et al. Nanoparticles functionalised with an anti-platelet human antibody for in vivo detection of atherosclerotic plaque by magnetic resonance imaging. Nanomedicine. 2015; 11:927–937. [PubMed: 25684334]
137. Zimmermann TS, Lee AC, Akinc A, Bramlage B, Bumcrot D, Fedoruk MN, Harborth J, Heyes JA, Jeffs LB, John M. RNAi-mediated gene silencing in non-human primates. Nature. 2006; 441:111–114. [PubMed: 16565705]
138. Shimada YJ, Cannon CP. PCSK9 (Proprotein convertase subtilisin/kexin type 9) inhibitors: past, present, and the future. Eur Heart J. 2015; 36:2415–2424. [PubMed: 25971287]
139. Giunzioni I, Tavori H, Covarrubias R, Major AS, Ding L, Zhang Y, DeVay RM, Hong L, Fan D, Predazzi IM, et al. Local Effects of Human PCSK9 on the Atherosclerotic Lesion. J Pathol. 2015
140. Frank-Kamenetsky M, Grefhorst A, Anderson NN, Racie TS, Bramlage B, Akinc A, Butler D, Charisse K, Dorkin R, Fan Y, et al. Therapeutic RNAi targeting PCSK9 acutely lowers plasma cholesterol in rodents and LDL cholesterol in nonhuman primates. Proc Natl Acad Sci U S A. 2008; 105:11915–11920. [PubMed: 18695239]

141. Luthi AJ, Patel PC, Ko CH, Mutharasan RK, Mirkin CA, Thaxton CS. Nanotechnology for synthetic high-density lipoproteins. Trends Mol Med. 2010; 16:553–560. [PubMed: 21087901]
142. Navab M, Reddy ST, Van Lenten BJ, Fogelman AM. HDL and cardiovascular disease: atherogenic and atheroprotective mechanisms. Nat Rev Cardiol. 2011; 8:222–232. [PubMed: 21304474]
143. Gordon DJ, Rifkind BM. High-density lipoprotein--the clinical implications of recent studies. N Engl J Med. 1989; 321:1311–1316. [PubMed: 2677733]
144. Skajaa T, Cormode DP, Falk E, Mulder WJ, Fisher EA, Fayad ZA. High-density lipoprotein-based contrast agents for multimodal imaging of atherosclerosis. Arterioscler Thromb Vasc Biol. 2010; 30:169–176. [PubMed: 19815819]
145. Kaul S, Coin B, Hedayiti A, Yano J, Cercek B, Chyu KY, Shah PK. Rapid reversal of endothelial dysfunction in hypercholesterolemic apolipoprotein E-null mice by recombinant apolipoprotein A-I(Milano)-phospholipid complex. J Am Coll Cardiol. 2004; 44:1311–1319. [PubMed: 15364338]
146. Luthi AJ, Lyssenko NN, Quach D, McMahon KM, Millar JS, Vickers KC, Rader DJ, Phillips MC, Mirkin CA, Thaxton CS. Robust passive and active efflux of cellular cholesterol to a designer functional mimic of high density lipoprotein. J Lipid Res. 2015; 56:972–985. [PubMed: 25652088]
147. Degoma EM, Rader DJ. Novel HDL-directed pharmacotherapeutic strategies. Nat Rev Cardiol. 2011; 8:266–277. [PubMed: 21243009]
148. Shaw JA, Bobik A, Murphy A, Kanellakis P, Blombery P, Mukhamedova N, Woollard K, Lyon S, Sviridov D, Dart AM. Infusion of reconstituted high-density lipoprotein leads to acute changes in human atherosclerotic plaque. Circ Res. 2008; 103:1084–1091. [PubMed: 18832751]
149. Duivenvoorden R, Tang J, Cormode DP, Mieszawska AJ, Izquierdo-Garcia D, Ozcan C, Otten MJ, Zaidi N, Lobatto ME, van Rijs SM. A statin-loaded reconstituted high-density lipoprotein nanoparticle inhibits atherosclerotic plaque inflammation. Nature communications. 2014:5.
150. Ross R. Atherosclerosis--an inflammatory disease. N Engl J Med. 1999; 340:115–126. [PubMed: 9887164]
151. Armitage J, Bowman L, Wallendszus K, Bulbulia R, Rahimi K, Haynes R, Parish S, Peto R, et al. Study of the Effectiveness of Additional Reductions in C, Homocysteine Collaborative G. Intensive lowering of LDL cholesterol with 80 mg versus 20 mg simvastatin daily in 12,064 survivors of myocardial infarction: a double-blind randomised trial. Lancet. 2010; 376:1658–1669. [PubMed: 21067805]
152. Rabar S, Harker M, O'Flynn N, Wierzbicki AS, Guideline Development G. Lipid modification and cardiovascular risk assessment for the primary and secondary prevention of cardiovascular disease: summary of updated NICE guidance. BMJ. 2014; 349:g4356. [PubMed: 25035388]
153. Ridker PM, Luscher TF. Anti-inflammatory therapies for cardiovascular disease. Eur Heart J. 2014; 35:1782–1791. [PubMed: 24864079]
154. Asai K, Funaki C, Hayashi T, Yamada K, Naito M, Kuzuya M, Yoshida F, Yoshimine N, Kuzuya F. Dexamethasone-induced suppression of aortic atherosclerosis in cholesterol-fed rabbits. Possible mechanisms. Arterioscler Thromb. 1993; 13:892–899. [PubMed: 8499410]
155. Van Put DJ, Van Hove CE, De Meyer GR, Wuyts F, Herman AG, Bult H. Dexamethasone influences intimal thickening and vascular reactivity in the rabbit collared carotid artery. Eur J Pharmacol. 1995; 294:753–761. [PubMed: 8750742]
156. Chono S, Tauchi Y, Deguchi Y, Morimoto K. Efficient drug delivery to atherosclerotic lesions and the antiatherosclerotic effect by dexamethasone incorporated into liposomes in atherogenic mice. J Drug Target. 2005; 13:267–276. [PubMed: 16051539]
157. Lobatto ME, Fayad ZA, Silvera S, Vucic E, Calcagno C, Mani V, Dickson SD, Nicolay K, Banciu M, Schiffelers RM. Multimodal clinical imaging to longitudinally assess a nanomedical anti-inflammatory treatment in experimental atherosclerosis. Molecular pharmaceutics. 2010; 7:2020–2029. [PubMed: 21028895]
158. Czock D, Keller F, Rasche FM, Haussler U. Pharmacokinetics and pharmacodynamics of systemically administered glucocorticoids. Clin Pharmacokinet. 2005; 44:61–98. [PubMed: 15634032]

159. Lobatto ME, Calcagno C, Otten MJ, Millon A, Ramachandran S, Paridaans MP, van der Valk FM, Storm G, Stroes ES, Fayad ZA, et al. Pharmaceutical development and preclinical evaluation of a GMP-grade anti-inflammatory nanotherapy. Nanomedicine. 2015; 11:1133–1140. [PubMed: 25791805]

160. van der Valk FM, van Wijk DF, Lobatto ME, Verberne HJ, Storm G, Willems MC, Legemate DA, Nederveen AJ, Calcagno C, Mani V. Prednisolone-containing liposomes accumulate in human atherosclerotic macrophages upon intravenous administration. Nanomedicine: Nanotechnology, Biology and Medicine. 2015; 11:1039–1046.

161. Schiener M, Hossann M, Viola JR, Ortega-Gomez A, Weber C, Lauber K, Lindner LH, Soehnlein O. Nanomedicine-based strategies for treatment of atherosclerosis. Trends Mol Med. 2014; 20:271–281. [PubMed: 24594264]

162. Scharlach C, Kratz H, Wiekhorst F, Warmuth C, Schnorr J, Genter G, Ebert M, Mueller S, Schellenberger E. Synthesis of acid-stabilized iron oxide nanoparticles and comparison for targeting atherosclerotic plaques: Evaluation by MRI, quantitative MPS, and TEM alternative to ambiguous Prussian blue iron staining. Nanomedicine: Nanotechnology, Biology and Medicine. 2015; 11:1085–1095.

163. Cheng D, Li X, Zhang C, Tan H, Wang C, Pang L, Shi H. Detection of Vulnerable Atherosclerosis Plaques with a Dual-Modal Single-Photon-Emission Computed Tomography/Magnetic Resonance Imaging Probe Targeting Apoptotic Macrophages. ACS applied materials & interfaces. 2015; 7:2847–2855. [PubMed: 25569777]

164. El-Dakdouki MH, El-Boubbou K, Kamat M, Huang R, Abela GS, Kiupel M, Zhu DC, Huang X. CD44 targeting magnetic glyconanoparticles for atherosclerotic plaque imaging. Pharm Res. 2014; 31:1426–1437. [PubMed: 23568520]

165. Qin H, Zhou T, Yang S, Chen Q, Xing D. Gadolinium (III)-gold nanorods for MRI and photoacoustic imaging dual-modality detection of macrophages in atherosclerotic inflammation. Nanomedicine. 2013; 8:1611–1624. [PubMed: 23351094]

166. Yilmaz A, Dengler MA, van der Kuip H, Yildiz H, Rösch S, Klumpp S, Klingel K, Kandolf R, Helluy X, Hiller K-H. Imaging of myocardial infarction using ultrasmall superparamagnetic iron oxide nanoparticles: a human study using a multi-parametric cardiovascular magnetic resonance imaging approach. European heart journal. 2013; 34:462–475. [PubMed: 23103659]

167. Tsuchiya K, Nitta N, Sonoda A, Nitta-Seko A, Ohta S, Takahashi M, Murata K, Mukaisho K, Shiomi M, Tabata Y. Evaluation of atherosclerotic lesions using dextran-and mannan-dextran-coated USPIO: MRI analysis and pathological findings. International journal of nanomedicine. 2012; 7:2271. [PubMed: 22619561]

168. Uchida M, Kosuge H, Terashima M, Willits DA, Liepold LO, Young MJ, McConnell MV, Douglas T. Protein cage nanoparticles bearing the LyP-1 peptide for enhanced imaging of macrophage-rich vascular lesions. ACS nano. 2011; 5:2493–2502. [PubMed: 21391720]

169. Terashima M, Uchida M, Kosuge H, Tsao PS, Young MJ, Conolly SM, Douglas T, McConnell MV. Human ferritin cages for imaging vascular macrophages. Biomaterials. 2011; 32:1430–1437. [PubMed: 21074263]

170. Kosuge H, Sherlock SP, Kitagawa T, Terashima M, Barral JK, Nishimura DG, Dai H, McConnell MV. FeCo/graphite nanocrystals for multi-modality imaging of experimental vascular inflammation. PloS one. 2011; 6:e14523–e14523. [PubMed: 21264237]

171. Morishige K, Kacher DF, Libby P, Josephson L, Ganz P, Weissleder R, Aikawa M. High-resolution magnetic resonance imaging enhanced with superparamagnetic nanoparticles measures macrophage burden in atherosclerosis. Circulation. 2010; 122:1707–1715. [PubMed: 20937980]

172. Maiseyeu A, Mihai G, Roy S, Kherada N, Simonetti OP, Sen CK, Sun Q, Parthasarathy S, Rajagopalan S. Detection of macrophages via paramagnetic vesicles incorporating oxidatively tailored cholesterol ester: an approach for atherosclerosis imaging. Nanomedicine. 2010; 5:1341–1356. [PubMed: 21128718]

173. Maiseyeu A, Mihai G, Kampfrath T, Simonetti OP, Sen CK, Roy S, Rajagopalan S, Parthasarathy S. Gadolinium-containing phosphatidylserine liposomes for molecular imaging of atherosclerosis. Journal of lipid research. 2009; 50:2157–2163. [PubMed: 19017616]

174. SHARMA G, SHE Z-G, VALENTA DT, STALLCUP WB, SMITH JW. Targeting of macrophage foam cells in atherosclerotic plaque using oligonucleotide-functionalized nanoparticles. Nano Life. 2010; 1:207. [PubMed: 23125876]
175. Kamat M, El-Boubbou K, Zhu DC, Lansdell T, Lu X, Li W, Huang X. Hyaluronic acid immobilized magnetic nanoparticles for active targeting and imaging of macrophages. Bioconjugate chemistry. 2010; 21:2128–2135. [PubMed: 20977242]
176. Sosnovik DE, Nahrendorf M, Deliolanis N, Novikov M, Aikawa E, Josephson L, Rosenzweig A, Weissleder R, Ntziachristos V. Fluorescence tomography and magnetic resonance imaging of myocardial macrophage infiltration in infarcted myocardium in vivo. Circulation. 2007; 115:1384–1391. [PubMed: 17339546]
177. Jaffer FA, Nahrendorf M, Sosnovik D, Kelly KA, Aikawa E, Weissleder R. Cellular imaging of inflammation in atherosclerosis using magnetofluorescent nanomaterials. Molecular imaging. 2006; 5:85. [PubMed: 16954022]
178. Pande AN, Kohler RH, Aikawa E, Weissleder R, Jaffer FA. Detection of macrophage activity in atherosclerosis in vivo using multichannel, high-resolution laser scanning fluorescence microscopy. Journal of biomedical optics. 2006; 11 021009-021009-021007.
179. Getts DR, Terry RL, Getts MT, Deffrasnes C, Müller M, van Vreden C, Ashhurst TM, Chami B, McCarthy D, Wu H. Therapeutic inflammatory monocyte modulation using immune-modifying microparticles. Science translational medicine. 2014; 6 219ra217-219ra217.
180. Bartneck M, Peters FM, Warzecha KT, Bienert M, van Bloois L, Trautwein C, Lammers T, Tacke F. Liposomal encapsulation of dexamethasone modulates cytotoxicity, inflammatory cytokine response, and migratory properties of primary human macrophages. Nanomedicine: nanotechnology, biology and medicine. 2014; 10:1209–1220.
181. Kosuge H, Sherlock SP, Kitagawa T, Dash R, Robinson JT, Dai H, McConnell MV. Near infrared imaging and photothermal ablation of vascular inflammation using single-walled carbon nanotubes. Journal of the American Heart Association. 2012; 1:e002568. [PubMed: 23316318]
182. Bruckman MA, Jiang K, Simpson EJ, Randolph LN, Luyt LG, Yu X, Steinmetz NF. Dual-modal magnetic resonance and fluorescence imaging of atherosclerotic plaques in vivo using VCAM-1 targeted tobacco mosaic virus. Nano Lett. 2014; 14:1551–1558. [PubMed: 24499194]
183. Winter PM, Neubauer AM, Caruthers SD, Harris TD, Robertson JD, Williams TA, Schmieder AH, Hu G, Allen JS, Lacy EK, et al. Endothelial alpha(v)beta3 integrin-targeted fumagillin nanoparticles inhibit angiogenesis in atherosclerosis. Arterioscler Thromb Vasc Biol. 2006; 26:2103–2109. [PubMed: 16825592]
184. Sanchez-Gaytan BL, Fay F, Lobatto ME, Tang J, Ouimet M, Kim Y, van der Staay SE, van Rijs SM, Priem B, Zhang L. HDL-Mimetic PLGA Nanoparticle To Target Atherosclerosis Plaque Macrophages. Bioconjugate chemistry. 2015; 26:443–451. [PubMed: 25650634]
185. Sigalov AB. Nature-inspired nanoformulations for contrast-enhanced in vivo MR imaging of macrophages. Contrast media & molecular imaging. 2014; 9:372–382. [PubMed: 24729189]
186. Cormode DP, Roessl E, Thran A, Skajaa T, Gordon RE, Schlomka J-P, Fuster V, Fisher EA, Mulder WJ, Proksa R. Atherosclerotic plaque composition: Analysis with multicolor CT and targeted gold nanoparticles1. Radiology. 2010
187. Cormode DP, Chandrasekar R, Delshad A, Briley-Saebo KC, Calcagno C, Barazza A, Mulder WJ, Fisher EA, Fayad ZA. Comparison of synthetic high density lipoprotein (HDL) contrast agents for MR imaging of atherosclerosis. Bioconjugate chemistry. 2009; 20:937–943. [PubMed: 19378935]
188. Chen W, Vucic E, Leupold E, Mulder WJ, Cormode DP, Briley-Saebo KC, Barazza A, Fisher EA, Dathe M, Fayad ZA. Incorporation of an apoE-derived lipopeptide in high-density lipoprotein MRI contrast agents for enhanced imaging of macrophages in atherosclerosis. Contrast media & molecular imaging. 2008; 3:233–242. [PubMed: 19072768]

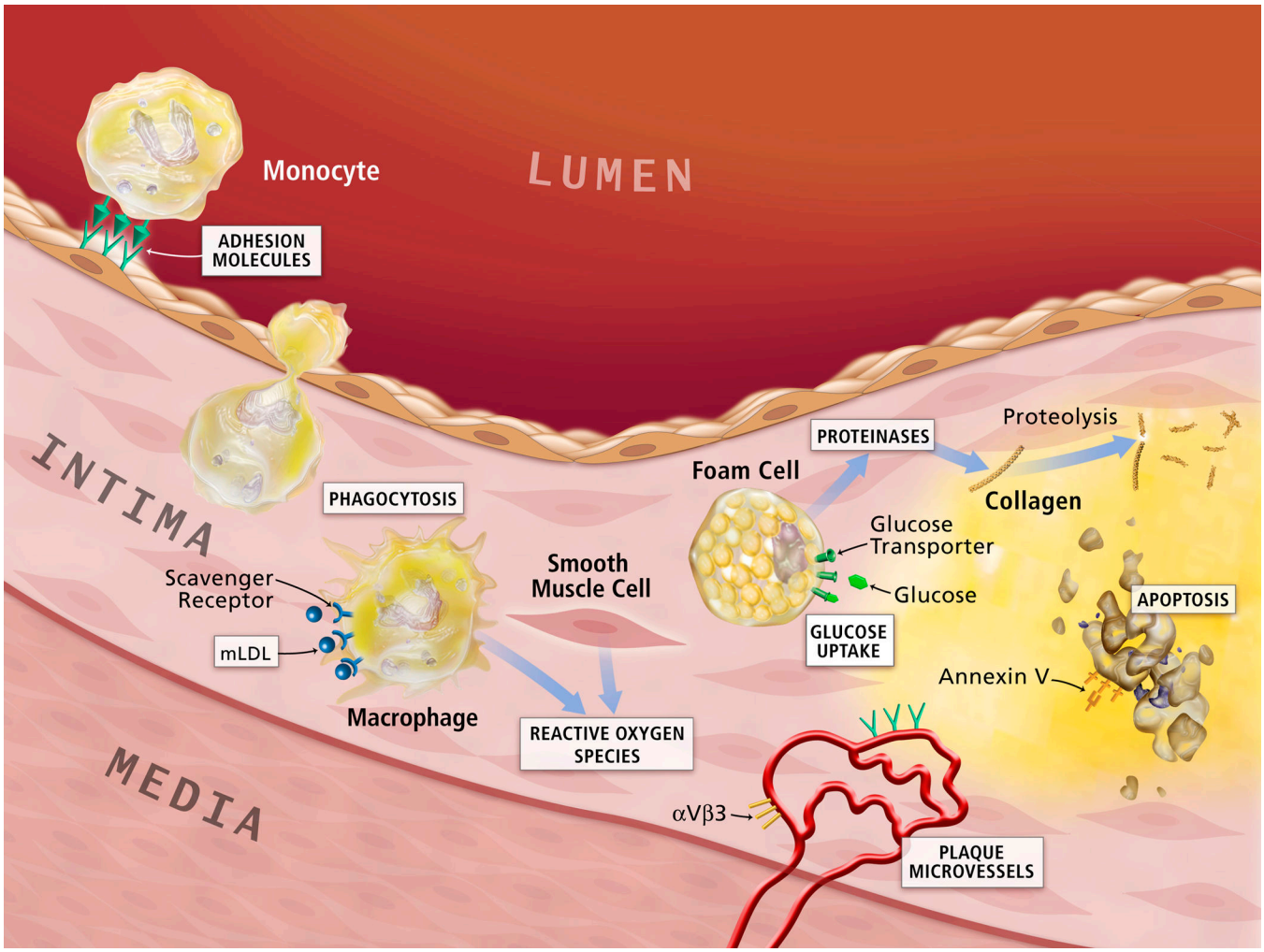

Figure 1. Potential lesion targets for detection and treatment of atherosclerosis

Nanoparticles can target to the specific cells or processes in the atherosclerotic lesions. The molecular or functional targets include macrophage scavenger receptors, macrophage phagocytosis, reactive oxygen species, proteases, annexin V for apoptosis, αvβ3 for neoangiogenesis, adhesion molecules and others. (Figure adapted and reprinted with the permission from reference, page 35S).

(Libby P, DiCarli M, Weissleder R. The vascular biology of atherosclerosis and imaging targets. J Nucl Med. 2010 May 1;51 Suppl 1:33S-37S.)

Table 1

Detection of atherosclerosis using macrophage-targeted nanoparticles

Molecular/ functional target	Nanoparticles	Imaging platforms	Animal model/patients, dose and administration route	Results	Year and reference
Macrophage phagocytosis	VSOPs electrostatically stabilized with malic acid, tartaric acid, etidronic acid, citric acid and dimercaptosuccinic acid (DMSA)	Magnetic particle spectroscopy (MPS), TEM, MRI	ApoE−/− mice; Fe 500 μmol/kg; I.V.	All four types of stabilized VSOPs accumulated in atherosclerotic lesions of apoE−/− mice, except that VSOPs coated by DMSA in myocardium; These four VSOPs accumulated in phagolysosomes of altered endothelial cells and macrophages in lesions; Citrate-coated VSOPs accumulation around 3-fold higher than malic, tartaric, etidronic acid-coated VSOPS in lesions.	2015[162]
Macrophage phagocytosis	USPIOs coated by carboxylated PEG and aminated PEG loaded with annexin V	MRI/SPECT	ApoE−/− mice; 18.5 MBq per mouse of ^{99m}Tc (Technetium) labeled USPIO−Annexin V; I.V.	Nanoparticle system (annexin V-hybrid) specifically targeted the vulnerable atherogenic lesions containing apoptotic macrophages.	2015[163]
CD36	Liposome-like nanoparticles modified with oxidized phospholipids	Near infrared *in vivo* IVIS® fluorescence imaging system	LDLr−/− mice; 0.5 μmol total phospholipids per mouse; I.V.	High binding affinity of targeted nanoparticles for the oxLDL binding sites of the CD36 receptor on macrophages (*in vitro*); Higher accumulation of targeted than non-targeted nanoparticles in aortic lesions (*in vivo*); Targeted nanoparticles co-localized with macrophages and their CD36 receptors in aortic lesions (*in vivo*).	2015[27]
Macrophage phagocytosis	PEGylated dendrimer-entrapped Au nanoparticles (Au DENPs)	CT	ApoE −/− mice; Au 0.1 mol/L, 100 μL; I.V.	PEGylated Au DENPs accumulated in macrophages and dominantly in their lysosomes; PEGylated Au DENPs can be used to detect murine macrophages distribution by CT imaging in apoE−/− mice.	2014[25, 26]
LOX-1	^{131}I-labelled LOX-1-targeted USPIOs; ligand is LOX-1 antibody	MRI	ApoE−/− mice; 30 μCi of ^{131}I-labelled LOX-1-targeted or untargeted USPIOs; I.V.	High uptake of targeted USPIOs in only activated RAW264.7 *in vitro*; Targeted USPIOs accumulated in carotid atherosclerotic lesions, co-localized with LOX-1 of macrophages and characterized vulnerable atherosclerotic lesions *in vivo*.	2014[36]

Molecular/ functional target	Nanoparticles	Imaging platforms	Animal model/patients, dose and administration route	Results	Year and reference
CD44	Hyaluronan (HA) magnetic glyconanoparticles (HA-NPs)	MRI	Atherosclerotic rabbit; Fe 0.21 mg/kg of body weight; I.V.	Selectively high binding of HA-NPs to CD44; Low dose of HA-NPs was significantly effective.	2014[164]
Macrophage phagocytosis	Gd-gold nanorods (Gd-GNRs)	Photoacoustic imaging (PAI) and MRI	Mice	Precise morphology to quantify the infiltration area and invasion depth of macrophages in the arterial wall by intravascular PAI.	2013[165]
Macrophages in myocardial infarction	USPIOs	MRI	Patients with an acute myocardial infarction; 17 mL USPIOs containing 510 mg Fe; I.V.	USPIOs was used to characterize myocardial infarct pathology by detecting infiltrating macrophages.	2013[166]
MSR1	USPIOs modified with a peptidic ligand targeting MSR1	MRI	ApoE−/− mice; Fe 250 μmol/kg; I.V.	Higher accumulation of MSR1–targeted USPIOs in atherosclerotic lesions (3.5-fold, *P=0.01*) than non-targeted USPIOs; Detection of inflammatory lesions *in situ* by MSR1–targeted USPIOs.	2013[70]
Macrophage phagocytosis	Dextran-coated USPIOs (D-USPIO) and Mannan–dextran-coated USPIOs (DM-USPIOs)	MRI, MRA	Watanabe heritable hyperlipidemic rabbits; Fe, 0.08, 0.4, 0.8 mmol/kg; I.V.	DM-USPIO was better than D-USPIO in targeting atherosclerotic lesions at all doses by reduction in the signal-noise ratio.	2012[167]
OxLDL	Lipid-coated USPIO nanoparticles (LUSPIOs) modified with oxLDL antibody as ligand	MRI	ApoE−/− mice; Fe 3.9 mg/kg; I.V.	LUSPIOs enabled the detection and characterization of atherosclerotic lesions by targeting oxLDL/oxidation-specific epitopes.	2011[40]
Macrophage phagocytosis	Nanoparticles modified by the LyP-1 peptide as ligand labeled by Cy5.5	Maestro™ *in vivo* fluorescence imaging system	Carotid-ligated mice producing macrophage-rich vascular lesions; 8 nmol of Cy5.5 per mouse; I.V.	LyP-nanoparticles (protein cage) had high binding affinity to macrophages *in vitro* and *in vivo*; They detected macrophage-rich murine carotid lesions *in situ* and *ex vivo*	2011[168]
Macrophage phagocytosis	Human ferritin protein cages encapsulating magnetite nanoparticles or conjugated to Cy5.5	MRI and fluorescence imaging	FVB strain mice	Ferritin nanoparticles accumulated in macrophages in atherosclerotic carotids; They detected vulnerable atherosclerotic lesions.	2011[169]
Macrophage phagocytosis	Iron-cobalt (FeCo) core with a graphitic-carbon (GC) shell	MRI and fluorescence imaging	Carotid-ligated (left) FVB strain mice to creat	Strong signals of FeCo/GC-Cy5.5 were founded in the ligated left carotid arteries, but not in the right control	2011[170]

Molecular/ functional target	Nanoparticles	Imaging platforms	Animal model/patients, dose and administration route	Results	Year and reference
	conjugated to Cy5.5 to form FeCo/GC nanocrystals		macrophage-rich atherosclerotic lesions; 8 nmol of Cy5.5 per mouse; I.V.	carotid arteries (non-ligated); FeCo/GC nanocrystals were co-localized with macrophages in the ligated carotid.	
Macrophage phagocytosis	Monocrystalline iron oxide nanoparticles-47 (MION-47)	MRI	New zealand white rabbits after balloon injury; Fe 10 mg/kg, 40 mg Fe per rabbit; I.V.	Iron was accumulated in immunoreactive macrophages in atheromatous lesions; MION-47 enabled macrophage burden estimation, inflamed lesion identification, therapy-mediated monitor in atheromatous lesions under MRI.	2010[171]
Macrophage phagocytosis	Gd phosphatidylserine enriched liposomes (Gd-PS-liposomes) with/without oxidized cholesterol ester derivative (cholesterol-9-carboxynonanoate [9-CCN]) as ligand	MRI	Watanabe heritable hyperlipidemic (WHHL) rabbits, I.V.	More Gd-PS-liposomes with 9-CCN (targeted) were accumulated in macrophages than liposomes without 9-CCN (non-targeted); Gd-PS-liposomes with 9-CCN (targeted) were co-localized with arterial macrophages.	2010[172]
Macrophage phagocytosis	Gd phosphatidylserine (PS) enriched liposomes (Gd-PS-liposomes) or Gd-liposomes	MRI	RAW264.7 macrophages, ApoE−/− mice	RAW264.7 showed PS dependent uptake of liposomes with PS composition (2, 6, 12, and 20%) compared to control liposomes without PS (0%); Gd-PS-liposomes were co-localized in macrophages and accumulated in atherosclerotic lesions.	2010[173]
Macrophage phagocytosis	Nanoparticles with a 23-merpoly-Guanine (polyG) oligonucleotide	Fluorescence imaging system	*In vitro:* RAW264.7 and THP-1 derived macrophages; *ex vivo:* tissue sections of atherosclerotic lesion from apoE−/− mice	Oligonucleotide nanoparticles had a high binding affinity to RAW264.7 and THP-1 derived macrophages, foam cells (*in vitro*) and sections of atherosclerotic lesions (*ex vivo*).	2010[174]
CD44	Iron oxide based magnetic nanoparticles bearing hyaluronic acid	MRI	THP-1 derived macrophages	The uptake of nanoparticles was dependent on both CD44 and hyaluronic acid.	2010[175]
CD36	Gd-lipid nanoparticles modified with CD36 antibody as a ligand	MRI	Human aortic specimens (*ex vivo*); 1 mM Gd nanoparticles	CD36-targeted nanoparticles had a high binding affinity to macrophages; They improved detection and characterization of vulnerable	2009

Molecular/ functional target	Nanoparticles	Imaging platforms	Animal model/patients, dose and administration route	Results	Year and reference
				atherosclerotic lesions.	
Macrophages via targeting oxLDL extracellularly	Micelles containing gadolinium and murine (MDA2 and E06) or human (IK17) antibodies that bound oxidation-specific epitopes	MRI	ApoE−/− mice; micelles, Gd 0.075 mmol/kg ; I.V.	Micelles with antibody of MDA2 or IK17 significantly accumulated in the arterial wall at 72 hours and E06 micelles at 96 hours than adjacent muscle IgG micelles; MDA2, IK17, and E06 micelles accumulated in macrophages in atherosclerotic lesions; Free MDA2 competed with MDA2 micelles and decreased its MRI signal.	2008[41]
CD204	Gd immunomicelles modified with CD204 antibody as ligand	MRI and fluorescence imaging	ApoE−/− and wild type mice, I.V.	Targeted immunomicelles demonstrated a 79% increase in the signal intensity of aortic lesions compared with non-targeted micelles with only 34% increase in apoE −/− mice; They detected macrophage content in vulnerable lesions.	2007[71]
Macrophage phagocytosis	Magnetofluorescent iron oxide nanoparticle modified with Cy5.5	Fluorescence tomography and MRI	C57BL/6 mice with infracted myocardium; Fe 3 to 20 mg/kg; I.V.	Nanoparticles enabled imaging of myocardial macrophage infiltration under both MRI and fluorescence tomography.	2007[176]
CD204	Micelles conjugated with CD204 antibodies modified with quantum dot, rhodamine and Gd	MRI	ApoE−/− mice; Gd 0.075 mmol/kg; I.V.	Micelles detected macrophages in apoE−/− mice effectively by optical methods and molecular MRI; CD204-targeted micelles enhanced signals up to 200% compared with non-targeted micelles.	2007[37]
Macrophage phagocytosis	Dextran-coated near-infrared magnetofluorescent nanoparticles (MFNPs)	MRI and fluorescence imaging	ApoE−/− mice; Fe 15 mg/kg; I.V.	Dextranated MFNPs accumulated in macrophages; Detection of atheroma by MFNP deposition under MRI.	2006[177]
Macrophage phagocytosis	Near-infrared fluorescent (NIRF) magnetofluorescent nanoparticle (MFNP)	Laser scanning fluorescence microscopy (LSFM)	ApoE −/− mice	MFNP-enhanced carotid atheroma demonstrated a significant NIRF signal by multichannel LSFM; NIRF signals were co-localized with immunostained macrophages.	2006[178]
Macrophage phagocytosis	USPIOs	MRI	Patients; Fe 2.6 mg/kg; I.V.	USPIOs enabled detection of macrophages in predominantly rupture-prone and ruptured human atherosclerotic lesions by MRI.	2003

Notes:
Au, Aurum

ApoE$^{-/-}$, apolipoprotein E null
Cy5.5, near-infrared (IR) fluorescence dye
CT, computed tomography
FVB, Friend leukemia virus B
Fe, iron
Gd, gadolinium (Gd)
I.V., intravenous injection
LDLr$^{-/-}$: LDL receptor null
LOX-1: lectin-like oxidized LDL receptor-1
LyP-1, a nine residue peptide shown to target macrophages
MSR1, macrophage scavenger receptor 1
MBq, megabecquerel as unit of radioactivity
MRI, magnetic resonance imaging
PEG, polyethylene glycol
STEM, scanning transmission electron microscopy
TEM, transmission electron microscopy
USPIOs: ultrasmall superparamagnetic iron oxide nanoparticles
VSOPs, very small iron oxide particles
/kg: per kilogram body weight

Table 2

Treatment of atherosclerosis using macrophage-targeted nanoparticles.

Molecular/ functional target	Nanoparticles	Imaging platforms	Animal model/patients, dose and administration route	Results	Year and reference
Macrophage phagocytosis	PLGA- b –PEG nanoparticles encapsulating liver X receptor (LXR) agonist GW3965 (NP-LXR)	N/A	LDLr−/− mice; GW3965: 10 mg/kg; I.P.	NP-LXR significantly decreased inflammatory factor expression and increased LXR-target gene expression in macrophages compared to free GW3965 *in vitro* and *in vivo*; NP-LXR were co-localized with lesion macrophages and reduced the CD68-positive macrophage content in lesions (by 50%) without increasing triglycerides or total cholesterol in the plasma and liver.	2015
Monocytes/ macrophages	Immune-modifying nanoparticles (IMPs), derived from polystyrene, microdiamonds and biodegradable PLGA	N/A	C57BL/6 mice with myocardial infarction; nanoparticles 1.4 mg/kg; I.V.	IMPs were taken up by inflammatory monocytes; Negatively charged IMPs bound to inflammatory monocytes, directed them to the spleen for apoptosis.	2014[179]
Macrophage phagocytosis	Liposomal dexamethasone	N/A	*In vitro*: primary human macrophages	Dexamethasone-loaded liposomes Inhibited monocyte and macrophage migration, reduced proinflammatory cytokine secretion (specifically TNF, IL-1β, IL-6).	2014[180]
Macrophage phagocytosis	^{89}Zirconium-radiolabeling dextran nanoparticle (^{89}Zr-DNP) modified with a near-infrared fluorochrome for microscopy; DNP loaded with CCR 2 siRNA	PET/MRI/Fluorescence imaging	ApoE−/− mice; I.V.	DNP were taken up predominantly by monocytes/macrophages (76.7%) and other leukocytes (12.5%); High uptake of ^{89}Zr-DNP in the aortic root of apoE−/− mice; ^{89}Zr-DNP lesion signals were decreased by therapeutic silencing of CCR2; Hybrid MRI/PET DNP demonstrated assessment of atherosclerotic inflammation.	2013[77]
Macrophage phagocytosis	Single-walled carbon nanotubes (SWNT) modified by Cy5.5	N/A	Carotid-ligated mice to produce macrophage-rich atherosclerotic lesions; 8 nmol of Cy5.5 per mouse or 0.6 nmol of SWNT per mouse; I.V.	High signal intensity of SWNT was found in ligated carotids; SWNT-Cy5.5 were co-localized with atherosclerotic macrophages; Light (808 nm) induced apoptosis of macrophages in ligated carotid arteries containing SWNTs, but not in control arteries without light exposure or without SWNTs.	2012[181]

Molecular/ functional target	Nanoparticles	Imaging platforms	Animal model/patients, dose and administration route	Results	Year and reference
Phosphatidyl serine (PS) receptor	PS-presenting liposomes containing iron oxide	MRI	Rats; 150 μL of 0.06 M PS-presenting liposomes or PS-lacking liposomes; I.V.	PS-presenting liposomes upregulated macrophage mannose receptor—CD206, increased secretion of anti-inflammatory cytokines, downregulated proinflammatory cytokines.	2011[52]
Monocytes/ macrophages	Lipid nanoparticle-encapsulated CCR2-siRNA	CT	ApoE−/− mice; 0.5 mg/kg/day of CCR2 siRNA, twice a week for 3 weeks; I.V.	Nanoparticles were co-localized with monocytes, and prevented monocytes accumulation in inflammatory sites by degrading CCR2 mRNA; CCR2 RNA silencing decreased monocytes/macrophages number in atherosclerotic lesions, reduced infarct size after coronary artery occlusion.	2011[73]
MSR1	Nanoscale amphiphilic macromolecules composed of a sugar backbone and PEG loaded with liver X receptor agonist GW3965	N/A	Sprague Dawley rats	The nanoscale macromolecules decreased intimal cholesterol levels (macromolecule alone 50%; macromolecule-encapsulated GW3965 70%) and prevented retention of macrophage (macromolecule 92%; macromolecule-encapsulated GW3965 96%) compared to non-treated controls.	2011[89]
Macrophage phagocytosis	Liposomal prednisolone phosphate (L-PLP)	PET/CT/MRI	Rabbits; PLP, 15 mg/kg; I.V.	L-PLP demonstrated significant higher anti-inflammatory effects than free PLP;	2010[157]
Macrophage phagocytosis	Dextran coated iron oxide nanoparticles modified with a near infrared fluorescence dye (detection) and a potent chlorin-based photosensitizer (treatment)	MRI	ApoE−/− mice; Fe 10 mg/kg (detection); chlorin 65 mg/kg (treatment); I.V.	Nanoparticles were accumulated in macrophage-rich atherosclerotic lesions; Photosensitizer nanoparticles eradicated inflammatory macrophages, subsequently stabilized lesions.	2010
Macrophage phagocytosis	L-PLP	PET/CT/MRI	Rats and rabbits; Toxicokinetic and pharmacokinetics study in rats: weekly L-PLP 0.5, 2 or 8 mg/kg; daily PLP 15 or 60 mg/kg for 28 days; I.V. Pharmacokinetics and anti-inflammatory	L-PLP had improved pharmacokinetics in rats and rabbits; No toxic effects of L-PLP were observed in rats; L-PLP decreased inflammatory response on the blood vessel wall in atherosclerotic rabbits.	2015[159]

Molecular/ functional target	Nanoparticles	Imaging platforms	Animal model/patients, dose and administration route	Results	Year and reference
			effects in rabbits: 1 mg/kg or 10 mg/kg; I.V.		
Macrophage phagocytosis	L-PLP	PET/CT/MRI	Human subjects Pharmacokinetics : 0.375 mg/kg, 0.75 mg/kg or1.5 mg/kg; I.V. Lesion macrophage delivery: 1.5 mg/kg; I.V. Therapeutic efficacy: 1.5 mg/kg; I.V.	Nanoencapsulation increased plasma half-life of PLP; PLP was accumulated in 75% of the lesion macrophages; No anti-inflammatory effects on the arterial wall.	2015[160]

Notes:
ApoE−/−, apolipoprotein E null
CT, computed tomography
CCR 2, C-C chemokine receptor type 2
Cy5.5, near-infrared (IR) fluorescence dye
IL-1β, interleukin-1 beta
IL-6, interleukin 6
I.V., intravenous injection
MRI, magnetic resonance imaging
MSR1, macrophage scavenger receptor 1
N/A, not applicable
PLGA, poly(lactic-coglycolic) acid
PEG, polyethylene glycol
PET, positron emission tomography
PLP, prednisolone phosphate
L-PLP, liposomal prednisolone phosphate
siRNA, small (short) interfering RNA
TNF, tumor necrosis factors
/kg: per kilogram body weight

Table 3

Detection and treatment of atherosclerosis using endothelial cell- and angiogensis-targeted nanoparticles

Molecular/ functional target	Nanoparticles	Imaging platforms	Animal model/patients, dose and administration route	Results	Year and reference
VCAM-1	Plant viral nanoparticle with tobacco mosaic virus (VCAM-TMV)	MRI	ApoE−/− mice,10 mg/kg VCAM-TMV and PEG-TMV; I.V.	VCAM-TMV targeted atherosclerotic lesions and increased the detection limitation of MRI.	2014[182]
VCAM-1	PEG-USPIO-VCAM-1 peptide nanoparticles with P03011 as a contrast agent	MRI and surface-enhanced coherent anti-Stokes Raman scattering (SECARS)	ApoE−/− mice; *in vivo* MRI measurements injected with contrast agent P03011 and control PEG-USPIO; *ex vivo* SECARS conducted on sections of aortic root.	SECARS microscopy and high magnetic field MRI combined with nanoencapsulated P03011 as a contrast agent improved visualization of atherosclerotic lesions.	2012[38]
VCAM-1 and apoptosis	USPIOs-R832 (VCAM-1 targeting) USPIO-R826 (apoptosis targeting)	MRI	ApoE−/− mice; Fe 0.1 mmol /kg USPIO-R832 and USPIO- R826; I.V.	Targeting apoptosis and VCAM-1 could be achieved in 30 minutes after treatment.	2012[99]
Transmembrane protein: stabilin-2	Peptide CRTLTVRKC (S2P)-HGC-Cy5.5 nanoparticles (S2P-HGC-Cy5.5-NP)	Fluorescence molecular imaging	ApoE−/− mice;10 mg/kg S2P–HGC-Cy5.5-NP; I.V.	S2P–HGC-Cy5.5-NP specifically targeted stabilin-2 expressed on endothelial cells.	2011[103]
VCAM-1	VCAM-1 internalizing peptide-28 (VHPKQHR) nanoparticles (VINP28-NPs)	High resolution MRI	ApoE−/−mice; I.V.	Detection of endothelial activation and damage was achieved by VINP28-NPs-enhanced *ex vivo* MRI.	2007[109]
αvβ3-integrin	αvβ3-fumagillin nanoparticles	MRI	Rabbits, αvβ3-Fumagillin NP 30 μg/kg	Angiogenesis was inhibited by αvβ3-fumagillin-nanoparticles in rabbits.	2006[183]
VCAM-1	VCAM-1 internalizing peptide-28 (VHPKQHR) nanoparticles (VINP28-NPs)	MRI	Murine cardiac endothelial cells	VINP28 modified multimodal nanoparticles had a high binding affinity to endothelial cells expressing VCAM-1, but not smooth muscle cells and macrophages.	2006[102]

Molecular/ functional target	Nanoparticles	Imaging platforms	Animal model/patients, dose and administration route	Results	Year and reference
VCAM-1	VCAM-1 internalizing peptide-28 (VHPKQHR) nanoparticles (VINP28-NPs)	MRI and optical imaging	ApoE−/− mice; 5 nmol/L fluorochrome of VINP28-NPs; I.V.	VINP28-NPs detected endothelial cells and macrophages by targeting VCAM-1; VINP28-NPs enabled spatial monitoring of anti–VCAM-1 pharmacotherapy *in vivo*.	2006[101]
VCAM-1	Peptide VHSPNKK-modified magnetofluorescent nanoparticles (VNP)	MRI	ApoE−/− mice; 5 ng/50 μL mTNF-α to induce inflammatory model;10 nmol/L VCAM-1 peptide, VNP or control nanoparticles.	VNP detected VCAM-1 expressed endothelial cells; VNP were co-localized with VCAM-1 expressed cells in atherosclerotic lesions in apoE−/− mice.	2005[100]

Notes:
MCP-1, monocyte chemoattractant protein-1
IL-8, interleukin 8
VCAM-1, endothelial vascular adhesion molecule-1
MRI, magnetic resonance imaging
I.V., intravenous injection
BAECs, bovine aortic endothelial cells
TMV, tobacco mosaic virus
AP, atherosclerotic plaque-homing peptide
HGC, hydrophobically modified glycol chitosan
Cy5.5, near-infrared (IR) fluorescence dye
HA, hyaluronan
USPIOs, ultrasmall superparamagnetic iron oxide
PEG, polyethylene glycol
SECARS, surface-enhanced coherent anti-Stokes Raman scattering
FMT, fluorescence molecular tomography
PET, positron emission tomography
SPECT, single photon emission computed tomography

Table 4

Detection and treatment of atherosclerosis using targeted nanoparticles via proteolysis, apoptosis and thrombosis processes

Molecular/ functional target	Nanoparticles	Imaging platforms	Animal model, dose and administration route	Results	Year and reference
Activated platelets	Versatile ultrasmall super paramagnetic iron oxide (VUSPIO) nanoparticles with recombinant human IgG4 antibody	MRI	*In vitro* human platelets; *ex vivo* human aorta samples; ApoE −/− mice; 10 μg/mL of antibody; I.V.	Nanoparticles bound to activated platelets.	2015[136]
Fibrin	Fibrin-binding peptides conjugated iron oxide nanoparticle–micelles (FibPep-ION-Micelles)	Magnetic particle imaging (MPI)	Human clots incubated with FibPep-ION-Micelles *in vitro*	Nanoparticles bound to the blood clot and gave a high signal.	2013[134]
Collapse of mitochondrial membrane potential during apoptosis	Synthetic biodegradable HDL-nanoparticles quantum dots	Optical imaging-fluorescence microscopy	RAW 264.7 macrophages, Male Sprague–Dawley rats; I.V.	Both *in vivo* and *in vitro* data revealed the increased detection of apoptotic cells. Synthetic biodegradable HDL-nanoparticles quantum dots targeted the collapse of mitochondrial membrane potential during apoptosis.	2013[129]
Activated platelets	Versatile ultrasmall superparamagnetic iron oxide (VUSPIO) particles, coupled to an anti-human P-selectin antibody (VH10)	MRI	Human platelets and endothelial cells; ApoE−/− mice. I.V.	VH10 bound to human activated platelets and endothelial cells.	2011[135]
Phosphatidyl serine on apoptotic cells and macrophages	Annexin A5-conjugated micellar nanoparticles carrying multiple Gd-labeled lipids and fluorescent lipids	MRI Fluorescence imaging	*In vitro* T-lymphoma cell line (Jurkat cells) at a concentration of 1 mM total lipid of nanoparticles; ApoE−/− mice, 2.5 μmol lipids per mouse; I.V.	Annexin A5-conjugated micellar nanoparticles targeted to apoptotic cells, and they detected PS-presenting cells in atherosclerotic lesions in apoE−/− mice.	2010[128]
Fibrin	Clot-binding peptide cysteine-arginine-glutamic acid-lysine-alanine (CREKA) bound micelles loaded with an anticoagulant	Fluorescence imaging	ApoE−/− mice; 100 μL of 1 mM micelles; I.V.	Micelles bound to unstable lesions in apoE−/− mice; Hirulog-loaded micelles had high hirulog concentrations and anti-thrombin activity in lesions.	2009[133]

Molecular/ functional target	Nanoparticles	Imaging platforms	Animal model, dose and administration route	Results	Year and reference
	drug hirulog				
Protease	Polymeric nanoparticles containing a protease sensor	Fluorescence molecular tomography (FMT) and CT	ApoE−/− mice; 5 nmol of protease sensor; I.V.	High signal intensity of nanoparticles was detected in the artery wall.	2009[123]
Phosphatidyl serine on apoptotic cells	Annexin V conjugated superparmagnetic iron oxide particles (SPIONs)	MRI	Watanabe heritable hyperlipidemic rabbits; SPIONs containing 0.05 mg of iron, I.V.	Annexin V conjugated SPIONs targeted to atherosclerotic lesions, but not healthy blood vessels.	2007[127]
Fibrin	Fibrin targeted (via anti-fibrin antibodies) Gd-DTPA-PE nanoparticles	MRI	Blood clots incubation	Gd-DTPA-PE nanoparticles modified with anti-fibrin antibodies had a high binding affinity to thrombi.	2003[131]

Notes:
ApoE−/−, apolipoprotein E null
CD44, cell surface adhesion molecule
Cy5.5, near-infrared (IR) fluorescence dye
CT, computed tomography
DTPA, diethylene-triamine-pentaacetic acid
Fe, iron
Gd, gadolinium
HDL, high-density lipoprotein
I.V., intravenous injection
MBq, megabecquerel as unit of radioactivity
MRI, magnetic resonance imaging
PE, phosphatidylethanolamine
PEG, polyethylene glycol
SPIONs , superparmagnetic iron oxide particles

Table 5

Detection and treatment of atherosclerosis using HDL nanoparticles

Molecular/ functional target	Nanoparticles	Imaging platforms	Animal model, dose and administration route	Results	Year and reference
Macrophages	PLGA-HDL nanoparticles: a lipid/apolipoprotein coating and a PLGA core	N/A	ApoE−/− mice	PLGA-HDL nanoparticles accumulated in atherosclerotic lesions; PLGA-HDL nanoparticles were co-localized with lesion macrophages.	2015[184]
Macrophages	Reconstituted HDL (rHDL) loaded with statin or Gd	MRI	ApoE−/− mice; Gd 50 mmol/kg in rHDL, statin 15 mg/kg as low dose; statin 60 mg/kg as high dose; I.V.	Statin-rHDL accumulated in macrophages in atherosclerotic lesions; Lesion inflammation was inhibited by 3-month low-dose of statin-rHDL; Inflammation in advanced atherosclerotic lesions was significantly reduced by 1 week high-dose of statin-rHDL.	2014[149]
Macrophages	Gd-based contrast agents-HDL (GBCA-HDL) modified by oxidized apoA-I or its peptides as ligands	N/A	ApoE−/− mice	The oxidation of apoA-I or its peptides increased uptake of GBCA-HDL (2–3 times) by macrophage *in vitro*; GBCA-HDL with oxidized apoA-I or its peptides accumulated in macrophages in the lesions in apoE−/− mice.	2014[185]
Macrophages	HDL mimic nanoparticles containing core, quantum dots (QDs) coated with PLGA, cholesteryl oleate, and a phospholipid bilayer decorated with cations triphenylphosphonium (TPP), apoA-I mimetic peptide and PEG	Optical imaging	Rats; TPP-HDL-apoA-I-QD NPs; 80 μg/kg with respect to QD, 10 mg/kg with respect to total nanoparticles; I.V.	Nanoparticles improved reverse cholesterol transport in *in vitro* studies; Nanoparticles decreased plasma triglyceride concentrations in rats.	2013[129]
Macrophages	Au-HDL	Multicolor CT	ApoE−/− mice; Au 500 mg/kg; I.V.	Multicolor CT identified lesion composition; Au-HDL accumulated in aortic macrophages.	2010[186]
Macrophages	HDL nanoparticles (peptide mimic and replace apoA-I) labeled with Gd and rhodamine	MRI	ApoE−/− mice; Gd-micelles, 50 μmol/kg; I.V.	HDL nanoparticles improved cholesterol efflux from macrophages and were taken up by cells in a receptor-dependent manner; HDL nanoparticles detected lesion	2009[187]

Molecular/ functional target	Nanoparticles	Imaging platforms	Animal model, dose and administration route	Results	Year and reference
				macrophages in apoE−/− mice.	
Macrophages	rHDL modified with a carboxyfluoresceine-labeled apoE-derived lipopeptide, P2A2 (rHDL-P2A2) nanoparticles	MRI	ApoE−/− mice; Gd-rHDL-P2A2, 50 μmol/kg; I.V.	rHDL-P2A2 nanoparticles significantly enhanced atherosclerotic signals; rHDL-P2A2 nanoparticles were co-localized with macrophages in lesions.	2008[188]

Notes:
ApoE−/−, apolipoprotein E null
Au, Aurum
ApoA-I, apolipoprotein A-I
CT, computed tomography
Gd, gadolinium
HDL, high-density lipoprotein
I.V., intravenous injection
MRI, magnetic resonance imaging
PLGA, poly(lactic-coglycolic) acid
PEG, polyethylene glycol
/kg, per kg body weight
rHDL, reconstituted HDL